Available online at www.sciencedirect.com
SCIENCE DIRECT®
Journal of Sound and Vibration 288 (2005) 487–521
JOURNAL OF SOUND AND VIBRATION
www.elsevier.com/locate/jsvi

Calculating frequency response functions for uncertain systems using complex affine analysis

G. Manson*

Dynamics Research Group, Department of Mechanical Engineering, University of Sheffield, Mappin Street, Sheffield, S1 3JD, UK

Received 21 June 2004; accepted 5 July 2005
Available online 19 August 2005

Abstract

This paper is concerned with the effect of parametric uncertainty upon the response of mechanical systems. Two uncertainty propagation techniques are employed and compared against a benchmark based upon randomly scanning input parameter ranges. The first technique, complex interval analysis, is computationally very efficient but suffers from the issue of dependency which may result in large overestimation of the system response. The second technique, namely complex affine analysis, is presented here for the first time and it keeps track of variable dependencies throughout the calculation thus limiting overestimation, albeit at some computational expense. The methods are demonstrated on the problem of calculation of the frequency response functions of a simple lumped mass system with uncertain parameters for purposes of transparency of the presented ideas, although these ideas are equally applicable to more complex systems. It transpired that the complex affine analysis performed significantly better than its interval counterpart.

1. Introduction

It is clearly desirable to know the full range of responses which may be exhibited by an engineering structure; this desire becomes a necessity in safety-critical situations. Even when a suitable numerical model may be developed, the issue of uncertainty can make the task of

*Tel.: +44 114 222 7790; fax: +44 114 222 7890.
E-mail address: graeme.manson@sheffield.ac.uk.

0022-460X/$ - see front matter © 2005 Elsevier Ltd. All rights reserved.
doi:10.1016/j.jsv.2005.07.004

evaluating the complete range of possible responses extremely difficult and/or time-consuming. Uncertainty arises in all engineering situations through incomplete knowledge of geometric and material properties, structural loading and environmental conditions, to name but a few.

Traditionally, the approach has been to run the model a large number of times with the input parameters randomly drawn from their respective ranges. The resulting ranges for the output variables of interest may then be ascertained. There are two main problems with such an approach. The first problem is that an extremely large number of model runs are required for more than a few uncertain parameters. This number grows exponentially as the number of uncertain parameters increases. In any but the simplest numerical model this will become prohibitively time-consuming. The second problem is that this approach does not concentrate on the extreme events which, in safety-critical situations, are the very events about which knowledge is desired. Phrased differently, random scanning of the crisply bounded input parameter domains results in underestimation of the true range of possible structural responses.

Interval analysis was designed to alleviate such problems and has naturally been extended into the complex plane as required for many engineering problems. It requires only a single run (or at least drastically fewer runs) of an altered version of the numerical model and returns predicted ranges for the structural responses which are *guaranteed* to contain the complete range of possible responses.

The biggest problem associated with interval analysis is the well-documented issue of dependency whereby interval analysis is unable to account for relationships between variables and assumes them to be independent of one another with the result, in many situations, being a dramatic overestimation of the output parameter ranges. The problem of dependency is exacerbated when the problem moves from the real to the complex plane. Real affine analysis was developed over 10 years ago in order to address the issue of dependency whilst retaining simplicity and has proved to be a very successful alternative. In this work, affine analysis is extended into the complex plane in order to investigate whether similar success may be achieved for situations where complex arithmetic is required.

Although the majority of investigations into structures under dynamic loading are concerned with obtaining the eigenvalues, and possibly eigenvectors, of the structure, a much more valuable description of the dynamic behaviour of the structure is the frequency response function (FRF) which describes the relationship between a local excitation force applied at one location on the structure and the resulting response at another location. Essentially, the FRF returns information about the behaviour of the structure over a range of frequencies. In deterministic problems the response at a particular frequency for some forcing and response locations will simply be a single complex number, which is often plotted in terms of real and imaginary parts or in terms of amplitude and phase. If the model parameters are prone to uncertainty however, the response at a particular frequency will then be a range of complex numbers which, when combined with all other discrete frequencies in the range, result in lower and upper bounds on the components of the FRF: again, these components may be real and imaginary or amplitude and phase.

There have been previous attempts to calculate bounds on FRFs for models with uncertain parameters which are guaranteed to be conservative. Dessombz et al. [1] used an iterative algorithm based around interval arithmetic to calculate guaranteed FRFs for several mechanical systems. The FRF bounds were tight to the true solution but, although requiring significantly less operations than the random scanning benchmark, the technique still required a large number of

operations even for relatively simple systems. In his thesis [2], Moens developed a finite element FRF analysis technique based around interval arithmetic by considering a set translation of the modal superposition procedure. Due to dependency problems, interval arithmetic had to be substituted by a time-consuming optimisation approach to calculate the modal parameter ranges. Interval arithmetic was then employed in the subsequent stages of the procedure with attempts being made to limit the effects of dependency where possible. Again, the results were impressive for the structures under consideration but it was acknowledged by the author that the optimisation "forms the numerically most expensive part of the procedure".

There are alternative approaches which may be applicable to FRF analysis for uncertain structures but do not return guaranteed solutions, without an optimisation stage. Hanss [3] developed the transformation method, which is essentially an extension of Dong and Shah's vertex method for fuzzy numbers [4] whilst Wood et al. [5] presented an enhancement to Dong and Wong's Fuzzy Weighted Average (FWA) algorithm [6] to consider non-monotonic functions.

The aim of this paper is to present an approach to FRF analysis for structures with uncertain parameters based around a complex affine arithmetic framework. It is anticipated that the affine approach will avoid many of the dependency problems associated with interval arithmetic without having to resort to computationally expensive optimisation algorithms. In order to illustrate the ideas, the effect of uncertain parameters upon the frequency response functions of a two degree-of-freedom system is investigated. As the system is relatively simple, a discussion of how the ideas may be extended to more complex systems is included towards the end of the paper.

The layout of the paper is as follows. Sections 2 and 3 give details of real and complex interval analysis, respectively. Sections 4 and 5 do similar for real and complex affine analysis. Section 5 spends some time comparing the results of several basic operations in interval and affine arithmetic. Section 6 benchmarks the two techniques against a standard approach for the two-degree-of-freedom system. The paper concludes with some discussion in Section 7.

2. Interval analysis

Although there was some previous work in the area, it was the early work of Moore, [7], where implementation of interval arithmetic on digital computers was discussed, and [8], where the function bounding properties of intervals were considered, that seems to have been the springboard for much of the subsequent research in interval analysis. This early work was expanded and collected in Moore's excellent monograph [9], the first entirely devoted to interval analysis, which has since be updated [10].

One of the first hurdles with interval analysis concerns the multitude of notations which have been employed in the past. In order to address this issue a standardised notation has been proposed [11] and will be used here.

An interval number, $\mathbf{x}$, is an ordered pair of real numbers, $[\underline{x}, \overline{x}]$, with $\underline{x} \leqslant \overline{x}$ ($\underline{x}$ is termed the lower bound or infimum and $\overline{x}$ the upper bound or supremum). If $\underline{x} = \overline{x}$ this is variously termed a *degenerate*, *weak*, *thin* or *point* interval and is equivalent to a real number. The interval number, $\mathbf{x}$, is also a *set* of real numbers, x, such that $\underline{x} \leqslant x \leqslant \overline{x}$. This may all be written

$$\mathbf{x} = \{x \in \mathbb{R} \mid \underline{x} \leqslant x \leqslant \overline{x}\}. \tag{1}$$

It is a straightforward matter to incorporate the idea of interval vectors and matrices. An interval vector or *box* of dimension n, $\mathbf{x}$ is defined as

$$\mathbf{x} = \{x \in \mathbb{R}^n \mid \underline{x} \leqslant x \leqslant \overline{x}\}, \tag{2}$$

where $\underline{x}$ and $\overline{x}$ are real column vectors of length n. Note that the inequality $\underline{x} \leqslant \overline{x}$ means that each component of $\underline{x}$ is less than or equal to its counterpart in $\overline{x}$. It should also be noted that there is no notational difference between interval numbers and interval vectors; both use bold, lowercase letters and interval numbers are simply treated as one-dimensional interval vectors.

There is a change in notation for interval matrices with bold, uppercase letters being used. An $m \times n$ interval matrix, $\mathbf{A}$, is defined as

$$\mathbf{A} = \{A \in \mathbb{R}^{m \times n} \mid \underline{A} \leqslant A \leqslant \overline{A}\}. \tag{3}$$

Each matrix component, $\mathbf{A}_{rc} = [\underline{A_{rc}}, \overline{A_{rc}}], (r = 1, \ldots, m, c = 1, \ldots, n)$, will be an interval number.

Let $\mathbf{x}$ and $\mathbf{y}$ be interval numbers such that $\mathbf{x} = [\underline{x}, \overline{x}]$ and $\mathbf{y} = [\underline{y}, \overline{y}]$. The four basic arithmetic operations are simply defined as

$$\mathbf{x} + \mathbf{y} = [\underline{x}, \overline{x}] + [\underline{y}, \overline{y}] = [\underline{x} + \underline{y}, \overline{x} + \overline{y}], \tag{4}$$

$$\mathbf{x} - \mathbf{y} = [\underline{x}, \overline{x}] - [\underline{y}, \overline{y}] = [\underline{x} - \overline{y}, \overline{x} - \underline{y}], \tag{5}$$

$$\mathbf{x} \times \mathbf{y} = [\underline{x}, \overline{x}] \times [\underline{y}, \overline{y}] = [\min\{\underline{x}\,\underline{y}, \underline{x}\,\overline{y}, \overline{x}\,\underline{y}, \overline{x}\overline{y}\}, \max\{\underline{x}\,\underline{y}, \underline{x}\,\overline{y}, \overline{x}\,\underline{y}, \overline{x}\overline{y}\}] \tag{6}$$

and, if $0 \notin [\underline{y}, \overline{y}]$,

$$\mathbf{x}/\mathbf{y} = [\underline{x}, \overline{x}]/[\underline{y}, \overline{y}] = [\underline{x}, \overline{x}] \times [1/\overline{y}, 1/\underline{y}]. \tag{7}$$

The addition and subtraction operations extend directly to interval vectors and matrices assuming dimensional compatibility of the operands. Multiplication of two interval matrices is conducted in the same manner as for real matrices with the exception that each component multiplication is done using Eq. (6) and each addition using Eq. (4). The width of an interval, $\mathbf{x}$, is simply $\overline{x} - \underline{x}$.

Let $f(x)$ be a continuous unary operation on $\mathbb{R}$. The interval evaluation of the function over the interval $\mathbf{x}$ is

$$f(\mathbf{x}) = \left[\inf_{x \in \mathbf{x}}\{f(x)\}, \sup_{x \in \mathbf{x}}\{f(x)\}\right] \tag{8}$$

If the function is monotonic (e.g. $\exp^x$, or x^{2n+1}) then the interval evaluation is straightforward. If the function is monotonically increasing, the interval evaluation will be given by

$$f(\mathbf{x}) = [f(\underline{x}), f(\overline{x})] \tag{9}$$

and for monotonically decreasing functions,

$$f(\mathbf{x}) = [f(\overline{x}), f(\underline{x})]. \tag{10}$$

The above equations may also be used if the function is monotonic over the range of $\mathbf{x}$. If a function is not monotonic over the range of $\mathbf{x}$ it is perfectly acceptable to split the range into several sub-ranges over each of which the function is monotonic then calculate the union of the function's sub-range evaluation. However, it is usually a trivial matter, with knowledge of a function's behaviour to evaluate the function range without resorting to division of the interval

range. For example, consider $f(x) = x^{2n}$ where $0 \in \mathbf{x}$. Knowledge of the function allows the specification of the interval evaluation of this function over $\mathbf{x}$ as

$$f(\mathbf{x}) = [0, \max(|\underline{x}|, |\overline{x}|)^{2n}]. \tag{11}$$

Interval arithmetic has become an effective tool for obtaining guaranteed bounds on rounding errors and the effects on a system's output of uncertainties on the input parameters. However, the major hurdle to wider applicability is interval arithmetic's potential for severe overestimation of the ranges. The reason for this overestimation is that some of the algebraic laws which are valid for real numbers are not valid for interval numbers. Some of the laws hold in a weaker form for interval numbers. Muhanna and Mullen [12] summed up the algebraic properties of interval operations in two general rules:

1. Two arithmetic expressions that are equivalent in real arithmetic, are equivalent in interval arithmetic when each variable occurs only once on each side. In this case, both sides yield the true range of the expression (this was stated by Moore [9]).
2. If f and g are two arithmetical expressions that are equivalent in real arithmetic, then the inclusion $f(x) \subseteq g(x)$ holds, if every variable occurs only once in f.

The first rule means that the laws of commutativity and associativity hold for interval numbers:

$$\mathbf{x} + \mathbf{y} = \mathbf{y} + \mathbf{x}, \quad \mathbf{x} * \mathbf{y} = \mathbf{y} * \mathbf{x} \quad \text{(commutativity)}, \tag{12}$$

$$(\mathbf{x} + \mathbf{y}) + \mathbf{z} = \mathbf{x} + (\mathbf{y} + \mathbf{z}), \quad (\mathbf{x} * \mathbf{y}) * \mathbf{z} = \mathbf{x} * (\mathbf{y} * \mathbf{z}) \quad \text{(associativity)}. \tag{13}$$

The laws of additive and multiplicative cancellation and distributivity do not satisfy this first rule and it transpires that they do not hold, in general, for interval numbers. That said, the second rule means that the weaker laws of subcancellation and subdistributivity do hold:

$$0 \in \mathbf{x} - \mathbf{x} \quad \text{(additive subcancellation)}, \tag{14}$$

$$1 \in \mathbf{x}/\mathbf{x} \quad \text{(multiplicative subcancellation)}, \tag{15}$$

$$\mathbf{x} * (\mathbf{y} + \mathbf{z}) \subseteq (\mathbf{x} * \mathbf{y}) + (\mathbf{x} * \mathbf{z}) \quad \text{(subdistributivity)}. \tag{16}$$

The left-hand side of Eq. (16) will return the exact range of the expression whilst the right-hand side will only return the exact range of the expression under special circumstances: if $\mathbf{x}$ is a real number or if $\mathbf{y} * \mathbf{z} \geqslant 0$.

The breakdown of the distributivity and cancellation laws are examples of a wider phenomenon relating to interval arithmetic termed *dependency*. The problem arises when variables occur more than once in an interval expression and may lead to a gross overestimation of the true range, especially in iterative processes. Interval arithmetic is not capable of recognising multiple occurrences of the same variable and evaluates all the intervals as independent of each other. Dependency is the most common reason for interval arithmetic being discarded as a means of propagation of uncertainties in many situations. In some situations, the overestimation due to dependency may be lessened or even eradicated using the following recommendations: (1) reducing the number of occurrences of the variables via symbolic cancellation before evaluation of the intervals, (2) rewriting polynomial expressions in *nested* or *Horner* form and (3) rewriting the

expression in what Moore [9] termed the *centred form* for the particular intervals of interest. The above recommendations are useful for specific expression types but, in most situations, there is little that can be done to eradicate the overestimation due to the issue of dependency. Hansen [13] stated that the endpoints of an interval evaluation of a function would only be sharp (the same as the actual range) if they are computed using only one endpoint of each of the interval variables. This means that, if the endpoints are tracked through a calculation, the appearance of the lower *and* upper bounds of any interval variable means that the particular endpoint of the function evaluation will not be sharp.

Dependency is the most common reason for interval arithmetic being discarded as a means of propagation of uncertainties.

3. Complex interval analysis

Boche [14] extended the idea of interval arithmetic to the complex plane by choosing the Cartesian representation for complex numbers. It is a relatively straightforward process. $\mathbf{x}$ now represents a complex interval number $\mathbf{x}_r + \mathrm{i}\mathbf{x}_i$ where $\mathbf{x}_r$ and $\mathbf{x}_i$ are the real and imaginary interval components of the complex number. The components are then assumed to be independent of one another such that

$$\mathbf{x}_r = [\underline{x}_r, \overline{x}_r] = \{x_r \in \mathbb{R} \mid \underline{x}_r \leqslant x_r \leqslant \overline{x}_r\}, \tag{17}$$

$$\mathbf{x}_i = [\underline{x}_i, \overline{x}_i] = \{x_i \in \mathbb{R} \mid \underline{x}_i \leqslant x_i \leqslant \overline{x}_i\}. \tag{18}$$

The four basic arithmetic operations for interval complex numbers $\mathbf{x}$ and $\mathbf{y}$ are defined below

$$\begin{aligned}\mathbf{x} + \mathbf{y} &= ([\underline{x}_r, \overline{x}_r] + [\underline{y}_r, \overline{y}_r]) + \mathrm{i}([\underline{x}_i, \overline{x}_i] + [\underline{y}_i, \overline{y}_i]) \\ &= ([\underline{x}_r + \underline{y}_r, \overline{x}_r + \overline{y}_r]) + \mathrm{i}([\underline{x}_i + \underline{y}_i, \overline{x}_i + \overline{y}_i]),\end{aligned} \tag{19}$$

$$\begin{aligned}\mathbf{x} - \mathbf{y} &= ([\underline{x}_r, \overline{x}_r] - [\underline{y}_r, \overline{y}_r]) + \mathrm{i}([\underline{x}_i, \overline{x}_i] - [\underline{y}_i, \overline{y}_i]) \\ &= ([\underline{x}_r - \overline{y}_r, \overline{x}_r - \underline{y}_r]) + \mathrm{i}([\underline{x}_i - \overline{y}_i, \overline{x}_i - \underline{y}_i]),\end{aligned} \tag{20}$$

$$\mathbf{x}\mathbf{y} = (\mathbf{x}_r\mathbf{y}_r - \mathbf{x}_i\mathbf{y}_i) + \mathrm{i}(\mathbf{x}_r\mathbf{y}_i + \mathbf{x}_i\mathbf{y}_r) \tag{21}$$

and if $0 \notin (\mathbf{y}_r^2 + \mathbf{y}_i^2)$

$$\frac{\mathbf{x}}{\mathbf{y}} = \frac{\mathbf{x}\mathbf{y}^*}{\mathbf{y}\mathbf{y}^*} = \frac{(\mathbf{x}_r\mathbf{y}_r + \mathbf{x}_i\mathbf{y}_i) + \mathrm{i}(\mathbf{x}_i\mathbf{y}_r - \mathbf{x}_r\mathbf{y}_i)}{\mathbf{y}_r^2 + \mathbf{y}_i^2}, \tag{22}$$

where $*$ signifies the complex conjugate of the complex interval. In order to ensure that division is possible, it is necessary to define the product of a complex interval and its complex conjugate as the intervalised version of the product of a crisp (i.e. degenerate) complex number and its complex conjugate:

$$\mathbf{y}\mathbf{y}^* = \mathbf{y}_r^2 + \mathbf{y}_i^2. \tag{23}$$

The above equation may seem superfluous but it is necessary, as simply substituting $\mathbf{x}_r = \mathbf{y}_r$ and $\mathbf{x}_i = -\mathbf{y}_i$ into Eq. (21) will not, in general, result in a zero imaginary part. When the product $\mathbf{y}_r\mathbf{y}_i$ is

subtracted from itself using standard interval arithmetic, the dependency problem arises in the form of failure of the law of additive cancellation. However, the weaker law of sub-cancellation, given in Eq. (14), does hold.

On the subject of dependency, the basic operations for complex interval arithmetic given in Eqs. (19)–(22) will now be examined for any dependency problems. First, it is assumed that the real and imaginary components of $\mathbf{x}$ are independent of one another (similarly for the components of $\mathbf{y}$). If this is not the case, then there will be issues of dependency for *every* complex interval operation, as the complex interval framework is not designed to deal with such a situation. This will be investigated in Section 5.

So, assuming that the real and imaginary components of $\mathbf{x}$ and $\mathbf{y}$ are independent, examination of Eqs. (19) and (20) shows that there are no dependency problems with regard to the complex interval addition and subtraction operations. For both operations, the lower and upper bounds of the real part are calculated using only one of the bounds from $\mathbf{x}_r$ and one of the bounds from $\mathbf{y}_r$. Similarly, for the lower and upper bounds of the imaginary part, using only one of the bounds from $\mathbf{x}_i$ and one of the bounds from $\mathbf{y}_i$. These operations satisfy the first general rule relating to dependency, stated in the last section, which was stated in an alternative manner by Hansen [13].

A similar examination of the right-hand side of Eq. (21) shows that, although all four real and imaginary components arise in the expressions for the real and imaginary components of the product, no component occurs more than once in either product component. In dependency terms, this means that the first general rule is satisfied and, therefore, the bounds on the real and imaginary components returned by the complex interval multiplication operation will be sharp to the true ranges of the real and imaginary components. That said, there is a dependency issue relating to multiplication. As previously stated, the real and imaginary components of the product are both calculated from the same four real and imaginary components and, therefore, there will be a relationship between the components of the product. This is best illustrated with a numerical example.

Fig. 1 shows the true solution set of the multiplication of $([3,7]+\mathrm{i}[2,4])$ by $([9,11]-\mathrm{i}[2,4])$ as the area within the dashed line. The results of the interval arithmetic multiplication are shown as a solid box, $([31,93]+\mathrm{i}[-10,38])$, which, as expected, gives sharp bounds for the real and imaginary components. However, complex interval multiplication is not able to represent the dependency which arises *between* the real and imaginary components. For a single interval multiplication the lack of dependency information between the real and imaginary parts is unlikely to cause significant problems. The issue of greater importance is the effect of this assumption of independence if subsequent operations are performed using this variable.

The final of the four basic operations was division of two complex interval numbers. As stated previously, it is essential that the product of a complex interval and its complex conjugate be calculated as the sum of the interval's real component squared and its imaginary component squared. Examination of Eq. (22) shows that $\mathbf{y}_r$ and $\mathbf{y}_i$ occur in both the numerator and denominator of both the real and imaginary components of the complex interval division. This multiple occurrence of variables is not recognised within the complex interval framework resulting, in general, in an overestimation of the true range for the real and imaginary components. Again, this is best illustrated with a numerical example. Consider the division of $([3,7]+\mathrm{i}[2,4])$ by $([9,11]-\mathrm{i}[2,4])$. Fig. 2 shows the true solution set as the area within the dashed line and the complex interval division result as the considerably larger solid-lined box,

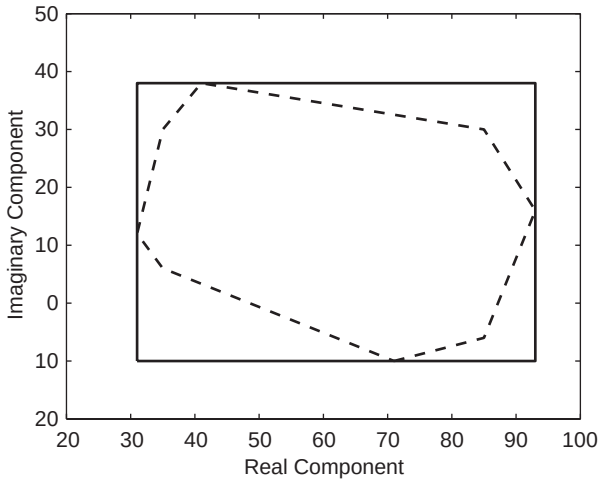

Fig. 1. Complex interval multiplication of $([3,7]+\mathrm{i}[2,4])$ by $([9,11]-\mathrm{i}([2,4])$ shown as solid box. True solution set boundary shown as dashed line.

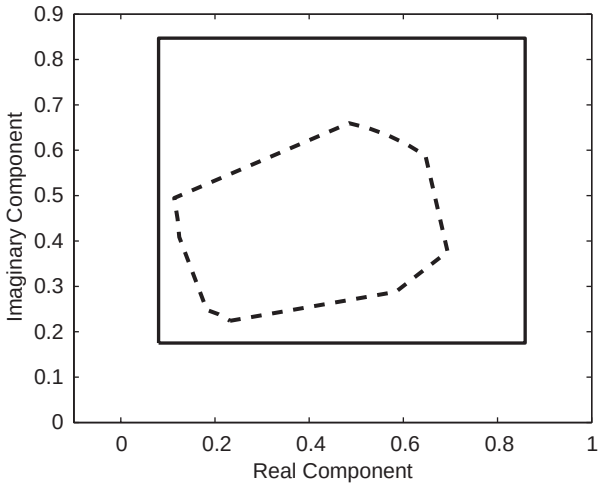

Fig. 2. Complex interval division of $([3,7]+\mathrm{i}[2,4])$ by $([9,11]-\mathrm{i}([2,4])$ shown as solid box. True solution set boundary shown as dashed line.

$([0.0803,0.8588]+\mathrm{i}([0.1752,0.8471])$. The overestimation of the complex interval approach is apparent.

It should be made clear that the issues of dependency arising through the use of the complex interval arithmetic operations which have been discussed above are *additional* sources of overestimation to those which are encountered in *all* interval arithmetic, as discussed in the last section.

The extension to complex interval vectors and matrices is a straightforward matter.

For the purpose of calculating the frequency response functions of the system of interest in Section 6, the basic arithmetic operations are sufficient.

4. Affine analysis

Affine analysis was first introduced in 1993 by Comba and Stolfi [15] where it was applied to computer graphics problems such as surface intersections. The basic idea of affine arithmetic is to keep track of dependency between operands and sub-formulae whilst retaining much of the simplicity of interval arithmetic. The result is that, in most situations, and certainly those where multiple iterations are necessary, affine arithmetic returns tighter bounds on the computed quantities than those obtained via interval arithmetic.

The notation which will be used in this paper is that from Comba and Stolfi's original paper [15] with a few, minor alterations and additions, aimed at making the proposed ideas more transparent.

In affine arithmetic, some partially uncertain parameter, x, is represented by an *affine form* $\hat{x}$, which is a first-order polynomial:

$$\hat{x} = x_0 + \sum_{i=1}^{n} x_i \varepsilon_i + x_{\text{err}} \varepsilon_{\text{err}}, \tag{24}$$

where x_i are known real coefficients and ε_i are symbolic variables whose values are unknown but lie in the range $[-1, 1]$. Each ε_i represents one of n independent sources of uncertainty whilst the corresponding coefficient x_i, termed *partial deviation*, gives the magnitude of that particular uncertainty. x_0 is termed the *central value*, for obvious reasons. The final term, $x_{\text{err}}\varepsilon_{\text{err}}$ is an approximation error term which is necessary as not all operations on affine forms result in an affine combination of the ε_i. ε_{err} is a completely new error symbol, treated as independent of all ε_i and lying in the range $[-1, 1]$, and x_{err} is an upper bound on the absolute difference between the true function and the affine approximation over the required range and will therefore always be non-negative.

It is straightforward to extend the idea to vectors and matrices of affine forms. In keeping with the notation for interval vectors and matrices, affine vectors will be specified using the same notation as affine forms, namely lowercase letters with a hat whilst affine matrices will be specified by uppercase letters with a hat.

It is often necessary, especially in the input and output of numerical programs and for comparison purposes, to convert between affine forms and intervals and vice versa. This is a straightforward process. Consider an affine form with an approximation error, as given in Eq. (24). This may be converted into an interval number, $\mathbf{x} = [\underline{x}, \overline{x}]$ where

$$\underline{x} = x_0 - \sum_{i=1}^{n} |x_i| - x_{\text{err}} \quad \text{and} \quad \overline{x} = x_0 + \sum_{i=1}^{n} |x_i| + x_{\text{err}}. \tag{25}$$

It should be stated that conversion from affine to interval forms results in the loss of all information regarding the interdependencies of parameters.

An interval number, $\mathbf{x} = [\underline{x}, \overline{x}]$, representing some quantity x may be converted into an equivalent affine form $\hat{x} = x_0 + x_{\text{new}}\varepsilon_{\text{new}}$ where

$$x_0 = \frac{\underline{x} + \overline{x}}{2}, \quad x_{\text{new}} = \frac{\overline{x} - \underline{x}}{2}. \tag{26}$$

Note that the error symbol ε_{new} will be distinct from all other ε symbols as the interval $\mathbf{x}$ contains no information regarding the source of uncertainty, only its overall width and the central value.

In order to illustrate affine arithmetic, let $\hat{x}$ and $\hat{y}$ be affine forms with approximation errors such that

$$\hat{x} = x_0 + \sum_{i=1}^{n} x_i\varepsilon_i + x_{\text{err}}\varepsilon_{\text{err}_x} \quad \text{and} \quad \hat{y} = y_0 + \sum_{i=1}^{n} y_i\varepsilon_i + y_{\text{err}}\varepsilon_{\text{err}_y}. \tag{27}$$

Certain arithmetic operations on real numbers (those that result in affine forms of the operands) will result in exact affine representations when extended to the case where the operands are affine forms whilst other operations will require the introduction of approximation terms. Examples of operations which return exact affine representations are addition, subtraction and scalar multiplication, addition and subtraction:

$$\hat{z} = \hat{x} \pm \hat{y} = (x_0 \pm y_0) + \sum_{i=1}^{n} (x_i \pm y_i)\varepsilon_i + (x_{\text{err}} + y_{\text{err}})\varepsilon_{\text{err}_z}, \tag{28}$$

$$\hat{z} = \alpha\hat{x} = \alpha x_0 + \sum_{i=1}^{n} \alpha x_i\varepsilon_i + \alpha x_{\text{err}}\varepsilon_{\text{err}_z}, \tag{29}$$

$$\hat{z} = \hat{x} \pm \alpha = (x_0 \pm \alpha) + \sum_{i=1}^{n} x_i\varepsilon_i + x_{\text{err}}\varepsilon_{\text{err}_z}, \tag{30}$$

where $\alpha \in \mathbb{R}$. Note that the ε_{err} term in the above equations have a z subscript to indicate that this is a new error symbol. It should also be noted from Eq. (28) that the partial deviation associated with the approximation error is $(x_{\text{err}} + y_{\text{err}})$ irrespective of whether addition or subtraction is being performed. The reason for this is because the assumed independent $\varepsilon_{\text{err}_x}$ and $\varepsilon_{\text{err}_y}$ terms are combined in a new $\varepsilon_{\text{err}_z}$ term whose partial deviation is guaranteed to contain the addition or subtraction of the previous terms.

The above operations extend directly to affine vectors and matrices assuming dimensional compatibility of the operands.

It is clear that most common mathematical operations may not be represented as affine combinations of their arguments. This means that the corresponding operations on affine forms will not result in affine combinations of the ε_i. The procedure for non-affine operations is to choose an affine function which gives a good approximation to the true function over the desired range then an approximation error term is added which is guaranteed to contain the maximum absolute difference between the affine function and the true function. Arguably the most common of the non-affine operations is multiplication, $z = x \times y$. Consider the product of affine forms $\hat{x}$

and $\hat{y}$ where the arguments are given in Eq. (27)

$$\begin{aligned} z^e = \hat{x} \times \hat{y} &= \left(x_0 + \sum_{i=1}^{n} x_i \varepsilon_i + x_{\mathrm{err}} \varepsilon_{\mathrm{err}_x} \right) \times \left(y_0 + \sum_{i=1}^{n} y_i \varepsilon_i + y_{\mathrm{err}} \varepsilon_{\mathrm{err}_y} \right) \\ &= x_0 y_0 + \sum_{i=1}^{n} (x_0 y_i + x_i y_0) \varepsilon_i + x_0 y_{\mathrm{err}} \varepsilon_{\mathrm{err}_y} + x_{\mathrm{err}} y_0 \varepsilon_{\mathrm{err}_x} \\ &\quad + \left(\sum_{i=1}^{n} x_i \varepsilon_i + x_{\mathrm{err}} \varepsilon_{\mathrm{err}_x} \right) \times \left(\sum_{i=1}^{n} y_i \varepsilon_i + y_{\mathrm{err}} \varepsilon_{\mathrm{err}_y} \right), \end{aligned} \tag{31}$$

where e denotes the exact expression. As stated previously, the aim is to approximate the above expression by an affine expression, termed z^a, plus a new approximation error term, $z_{\mathrm{err}} \varepsilon_{\mathrm{err}_z}$:

$$\hat{z} = z^a + z_{\mathrm{err}} \varepsilon_{\mathrm{err}_z}, \tag{32}$$

where

$$z_{\mathrm{err}} = \max\{|z^e - z^a|\} \quad \forall \varepsilon_1, \ldots, \varepsilon_n, \varepsilon_{\mathrm{err}_x}, \varepsilon_{\mathrm{err}_y} \in [-1, 1] \tag{33}$$

and $\varepsilon_{\mathrm{err}_z}$ lies in the range $[-1, 1]$. A quick, conservative affine estimate was suggested by Comba and Stolfi [15] for multiplication of two affine forms, without approximation errors. It is a simple matter to extend Comba and Stolfi's expression for affine forms with approximation errors. The affine approximation, z^a, is given by

$$z^a = x_0 y_0 + \sum_{i=1}^{n} (x_0 y_i + x_i y_0) \varepsilon_i \tag{34}$$

and the approximation error partial deviation, z_{err}, is given by

$$z_{\mathrm{err}} = |x_0| y_{\mathrm{err}} + x_{\mathrm{err}} |y_0| + \left(\sum_{i=1}^{n} |x_i| + x_{\mathrm{err}} \right) \times \left(\sum_{i=1}^{n} |y_i| + y_{\mathrm{err}} \right). \tag{35}$$

On many occasions the above estimate returns very conservative results. In Ref. [16] the author presented two further estimates which retained information, previously 'lost' in Comba and Stolfi's approximation error. The better estimate (and the one which will shortly be adapted for complex affine analysis) had an affine approximation, z^a, given by

$$z^a = \left(x_0 y_0 + \frac{1}{2} \sum_{i=1}^{n} x_i y_i \right) + \sum_{i=1}^{n} (x_0 y_i + x_i y_0) \varepsilon_i \tag{36}$$

and an approximation error partial deviation, z_{err}, given by

$$\begin{aligned} z_{\mathrm{err}} &= \frac{1}{2} \sum_{i=1}^{n} |x_i y_i| + \sum_{i=1}^{n} \sum_{j=i+1}^{n} |(x_i y_j + x_j y_i)| + x_{\mathrm{err}} y_{\mathrm{err}} \\ &\quad + \left[\left(|x_0| + \sum_{i=1}^{n} |x_i| \right) \times y_{\mathrm{err}} \right] + \left[x_{\mathrm{err}} \times \left(|y_0| + \sum_{i=1}^{n} |y_i| \right) \right]. \end{aligned} \tag{37}$$

The first improvement from the standard estimate is due to the realisation that the $x_i y_i \varepsilon_i^2$ terms arising from Eq. (31) will vary between 0 and $x_i y_i$ as opposed to $-x_i y_i$ and $x_i y_i$, as assumed by the Comba and Stolfi estimate. The second improvement arises from the realisation that by summing the $x_i y_j$ and $x_j y_i$ terms, as in Eq. (37), the magnitude of the contribution towards the overall approximation error may be less than the equivalent contribution assumed in Eq. (35), $|x_i||y_j| + |x_j||y_i|$.

The benefits of these reductions in approximation error will be most noticeable in matrix multiplications where the components of the matrices are affine forms with more than one independent source of uncertainty, although improvements may be observed in many multiplications of two affine forms.

Unlike multiplication, most other commonly used non-affine operations have only one operand e.g. e^x, x^n, $1/x$ and $\sqrt{x}$. The two common techniques for approximating these operations are the Chebyshev (or minimax) approximation and the min-range approximation. Both techniques, and their associated advantages and disadvantages, were discussed in Refs. [16,17] in some detail. In this work, only the Chebyshev approximations for the reciprocal function and the squared function are required and as such will be the only non-affine unary operations considered here.

The Chebyshev approximation for the operation $z = 1/x$ over an interval range $\mathbf{x} = [a, b]$ (note $0 \notin \mathbf{x}$) is given by

$$\hat{z} = \alpha\hat{x} + \beta + \delta\varepsilon_{\mathrm{err}_z} = \alpha\left(x_0 + \sum_{i=1}^{n} x_i\varepsilon_i + x_{\mathrm{err}}\varepsilon_{\mathrm{err}}\right) + \beta + \delta\varepsilon_{\mathrm{err}_z}, \tag{38}$$

where

$$\alpha = -\frac{1}{ab}, \quad \beta = \frac{1}{2a} + \frac{1}{2b} + \frac{1}{\sqrt{ab}}, \quad \delta = \left|\frac{1}{2a} + \frac{1}{2b} - \frac{1}{\sqrt{ab}}\right| \tag{39}$$

whilst the Chebyshev approximation for the operation $z = x^2$ over an interval range $\mathbf{x} = [a, b]$ has the same form as Eq. (38) with the parameters α, β and δ given by

$$\alpha = a + b, \quad \beta = -\frac{ab}{2} - \frac{(a+b)^2}{8}, \quad \delta = \left|\frac{ab}{2} - \frac{(a+b)^2}{8}\right|. \tag{40}$$

5. Complex affine analysis

In the same manner as affine analysis offers an alternative to interval analysis which is able to account for dependencies between real variables, in this section will be presented an alternative to complex interval analysis based around the framework of complex affine arithmetic.

There are a few possible approaches to the extension of affine arithmetic to the complex plane. The one proposed here allows for dependency between the real and imaginary components of a particular variable to be represented, something not possible using complex interval arithmetic. Separate real and imaginary approximation errors will be calculated. The thinking behind this decision is based upon several reasons: (1) the errors are essentially 'lost' to the calculation, and therefore representation of dependencies between real and imaginary errors is of little value, (2) it

is possible to represent a relatively large real error with a small imaginary error (and vice versa), something which would not be possible with a single error term and (3) easy visualisation of complex affine variables. Overall, it is expected that this decision to use separate real and imaginary errors will result in tighter bounds and more straightforward analysis than if a single error term were employed.

So, a complex affine approximation, with error terms, for some uncertain complex parameter, x, is given by (cf. Eq. (24) for a real parameter)

$$\hat{x} = x_0 + \sum_{i=1}^{n} x_i \varepsilon_i + x_{\text{real}} \varepsilon_{\text{real}} + \mathrm{i} x_{\text{imag}} \varepsilon_{\text{imag}}, \tag{41}$$

where x_0 and x_i are now known *complex* coefficients and ε_i are symbolic variables whose values are unknown but lie in the range $[-1, 1]$. As in the previous section, each of the ε_i represents one of n independent sources of uncertainty whilst the corresponding coefficient x_i, termed *partial deviation*, now gives the magnitude of that particular uncertainty in the real and imaginary directions. x_0, the central value, is now complex. Both x_{real} and x_{imag} are real and positive. $\varepsilon_{\text{real}}$ and $\varepsilon_{\text{imag}}$ represent the real and imaginary approximation errors respectively and are completely new error symbols, treated as independent of all ε_i and lying in the range $[-1, 1]$. x_{real} is the upper bound on the absolute difference between the real part of the true function and the real part of the affine approximation over the required range and will therefore always be non-negative. x_{imag} is the upper bound on the absolute difference between the imaginary parts and will therefore also be non-negative. Extension to complex affine vectors and matrices is straightforward.

As with real interval numbers and affine forms, it is often necessary to convert between complex affine forms and complex intervals and vice versa. This is straightforward. Consider a complex affine form with an approximation error, as given in Eq. (41). This may be converted to a complex interval number $\mathbf{x} = \mathbf{x}_r + \mathrm{i}\mathbf{x}_i = [\underline{x}_r, \overline{x}_r] + \mathrm{i}[\underline{x}_i, \overline{x}_i]$ where

$$\begin{aligned} \underline{x}_r &= \mathrm{Re}(x_0) - \sum_{i=1}^{n} |\mathrm{Re}(x_i)| - x_{\text{real}}, \quad \overline{x}_r = \mathrm{Re}(x_0) + \sum_{i=1}^{n} |\mathrm{Re}(x_i)| + x_{\text{real}}, \\ \underline{x}_i &= \mathrm{Im}(x_0) - \sum_{i=1}^{n} |\mathrm{Im}(x_i)| - x_{\text{imag}} \quad \text{and} \quad \overline{x}_i = \mathrm{Im}(x_0) + \sum_{i=1}^{n} |\mathrm{Im}(x_i)| + x_{\text{imag}}. \end{aligned} \tag{42}$$

Whilst conversion from real affine forms to real interval numbers resulted in the loss of all information regarding the interdependencies between parameters, conversion between complex affine forms and complex interval numbers potentially results in further loss of information. This loss is due to the assumption of independence of the real and imaginary components in complex interval analysis whereas dependency between the components is permissible in complex affine analysis. This is best illustrated by the example shown in Fig. 3. The complex affine number $\hat{x} = (10 + 5\mathrm{i}) + (3 + 2\mathrm{i})\varepsilon_1 + (-1 + \mathrm{i})\varepsilon_2 + 2\varepsilon_{\text{real}} + \mathrm{i}\varepsilon_{\text{imag}}$ is the solid-lined convex hull whilst the dotted line shows the conversion to the complex interval number $[4, 16] + \mathrm{i}[1, 9]$ whose bounds are calculated using Eq. (42). The loss of information is apparent.

A complex interval number, $\mathbf{x} = \mathbf{x}_r + \mathrm{i}\mathbf{x}_i = [\underline{x}_r, \overline{x}_r] + \mathrm{i}[\underline{x}_i, \overline{x}_i]$, representing some quantity x may be converted into an equivalent complex affine form $\hat{x} = x_0 + x_{\text{new}_1} \varepsilon_{\text{new}_1} + x_{\text{new}_2} \varepsilon_{\text{new}_2}$

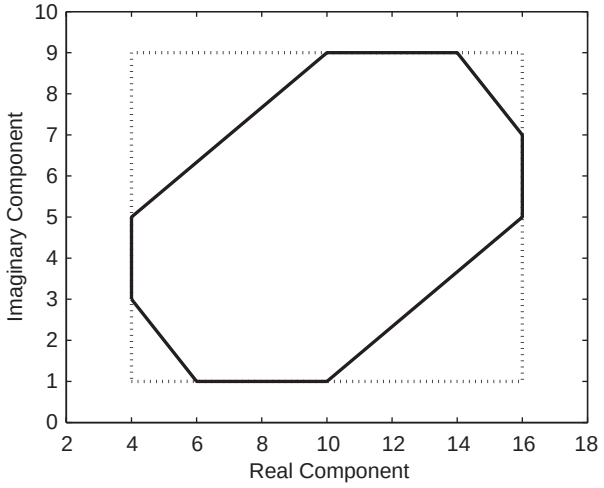

Fig. 3. Comparison of complex affine form (solid line) with complex interval conversion (dotted line).

where

$$x_0 = \frac{(\underline{x}_r + \overline{x}_r) + \mathrm{i}(\underline{x}_i + \overline{x}_i)}{2}, \quad x_{\mathrm{new}_1} = \frac{\overline{x}_r - \underline{x}_r}{2}, \quad x_{\mathrm{new}_2} = \frac{i(\overline{x}_i - \underline{x}_i)}{2}. \tag{43}$$

Note that, as $\mathbf{x}$, the complex interval number, represents a rectangle in the complex plane, it is necessary to introduce two new error symbols to represent the same rectangle in terms of a complex affine form. These error symbols, $\varepsilon_{\mathrm{new}_1}$ and $\varepsilon_{\mathrm{new}_2}$, will be distinct from all other ε symbols. There is no loss of information, or overestimation, when converting from a complex interval to a complex affine form. However, consider the effect of pre-converting the complex interval number $\mathbf{x} = [4, 16] + \mathrm{i}[1, 9]$ to a complex affine form. Using Eq. (43) gives $\hat{x} = (10 + 5\mathrm{i}) + 6\varepsilon_{\mathrm{new}_1} + 4\mathrm{i}\varepsilon_{\mathrm{new}_2}$. This may be compared to the complex affine form depicted as the convex hull in Fig. 3. The interval rectangle will be converted into an overlying affine rectangle as opposed to the convex hull from which the interval rectangle was initially converted.

As with real affine arithmetic, there are certain arithmetic operations in complex affine arithmetic which have exact affine representations whilst others require approximations. Let $\hat{x}$ and $\hat{y}$ be complex affine forms with approximation errors such that

$$\hat{x} = x_0 + \sum_{i=1}^{n} x_i\varepsilon_i + x_{\mathrm{real}}\varepsilon_{\mathrm{real}_x} + \mathrm{i}x_{\mathrm{imag}}\varepsilon_{\mathrm{imag}_x} \quad \text{and} \quad \hat{y} = y_0 + \sum_{i=1}^{n} y_i\varepsilon_i + y_{\mathrm{real}}\varepsilon_{\mathrm{real}_y} + \mathrm{i}y_{\mathrm{imag}}\varepsilon_{\mathrm{imag}_y}, \tag{44}$$

where the central values x_0 and y_0 and the partial deviations x_i and y_i are complex-valued. The error terms x_{real}, x_{imag}, y_{real} and y_{imag} are all real-valued.

The same operations which have exact affine representations for real affine forms have exact representations for complex affine forms. Addition and subtraction of two complex affine forms and multiplication, addition and subtraction of a complex scalar are

given by

$$\begin{aligned}\hat{z} &= \hat{x} \pm \hat{y} \\ &= (x_0 \pm y_0) + \sum_{i=1}^{n} (x_i \pm y_i)\varepsilon_i + (x_{\text{real}} + y_{\text{real}})\varepsilon_{\text{real}_z} + \text{i}(x_{\text{imag}} + y_{\text{imag}})\varepsilon_{\text{imag}_z},\end{aligned} \tag{45}$$

$$\begin{aligned}\hat{z} &= \alpha\hat{x} \\ &= \alpha x_0 + \sum_{i=1}^{n} \alpha x_i \varepsilon_i + (|\alpha_{\text{real}}|x_{\text{real}} + |\alpha_{\text{imag}}|x_{\text{imag}})\varepsilon_{\text{real}_z} + \text{i}(|\alpha_{\text{real}}|x_{\text{imag}} + |\alpha_{\text{imag}}|x_{\text{real}})\varepsilon_{\text{imag}_z},\end{aligned} \tag{46}$$

$$\hat{z} = \hat{x} \pm \alpha = (x_0 \pm \alpha) + \sum_{i=1}^{n} x_i \varepsilon_i + x_{\text{real}}\varepsilon_{\text{real}_z} + \text{i}x_{\text{imag}}\varepsilon_{\text{imag}_z}, \tag{47}$$

where $\alpha \in \mathbb{C}$. Note that the $\varepsilon_{\text{real}}$ and $\varepsilon_{\text{imag}}$ terms in the above equations have a z subscript to indicate that these are new error symbols. In a similar manner to the real affine operations, the partial deviations associated with the real and imaginary approximation errors in Eq. (45) are $(x_{\text{real}} + y_{\text{real}})$ and $(x_{\text{imag}} + y_{\text{imag}})$, respectively, irrespective of whether addition or subtraction is being performed. This is because the assumed independent $\varepsilon_{\text{real}_x}$ and $\varepsilon_{\text{real}_y}$ terms are combined in a new $\varepsilon_{\text{real}_z}$ term whose partial deviation is guaranteed to contain the addition or subtraction of the previous terms. The same is true for the imaginary approximation errors. A similar case arises for the approximation errors in Eq. (46) with the worst-case situation being assumed in order to guarantee conservatism.

The above operations extend directly to complex affine vectors and matrices assuming dimensional compatibility of the operands.

As was the case with the arithmetic for real affine forms, most operations on complex affine forms may not be represented by an affine combination of the ε_i and it becomes necessary to choose an affine function which is a good approximation to the actual function over the range of interest to which is added an approximation error which gives guaranteed containment of the true function. Again, the most common of the non-affine operations is, arguably, multiplication, $z = x \times y$. Consider the product of affine forms $\hat{x}$ and $\hat{y}$ where the arguments are given in Eq. (44):

$$\begin{aligned}z^e &= \hat{x} \times \hat{y} \\ &= \left(x_0 + \sum_{i=1}^{n} x_i\varepsilon_i + x_{\text{real}}\varepsilon_{\text{real}_x} + \text{i}x_{\text{imag}}\varepsilon_{\text{imag}_x}\right) \times \left(y_0 + \sum_{i=1}^{n} y_i\varepsilon_i + y_{\text{real}}\varepsilon_{\text{real}_y} + \text{i}y_{\text{imag}}\varepsilon_{\text{imag}_y}\right) \\ &= x_0y_0 + \sum_{i=1}^{n}(x_0y_i + x_iy_0)\varepsilon_i + x_0y_{\text{real}}\varepsilon_{\text{real}_y} + x_{\text{real}}y_0\varepsilon_{\text{real}_x} + \text{i}x_0y_{\text{imag}}\varepsilon_{\text{imag}_y} + \text{i}x_{\text{imag}}y_0\varepsilon_{\text{imag}_x} \\ &\quad + \left(\sum_{i=1}^{n} x_i\varepsilon_i + x_{\text{real}}\varepsilon_{\text{real}_x} + \text{i}x_{\text{imag}}\varepsilon_{\text{imag}_x}\right) \times \left(\sum_{i=1}^{n} y_i\varepsilon_i + y_{\text{real}}\varepsilon_{\text{real}_y} + \text{i}y_{\text{imag}}\varepsilon_{\text{imag}_y}\right),\end{aligned} \tag{48}$$

where e denotes the exact expression. The aim is to approximate the above expression by an affine expression, termed z^a, plus new real and imaginary approximation error terms, $z_{\text{real}}\varepsilon_{\text{real}_z}$ and $z_{\text{imag}}\varepsilon_{\text{imag}_z}$:

$$\hat{z} = z^a + z_{\text{real}}\varepsilon_{\text{real}_z} + \text{i}z_{\text{imag}}\varepsilon_{\text{imag}_z} \tag{49}$$

It is straightforward to derive a quick, conservative complex affine estimate of the form suggested by Comba and Stolfi [15] for multiplication of two real affine forms. The affine approximation, z^a, takes the same form as Eq. (34), but the coefficients, x_0, y_0, x_i and y_i, will be complex in this case

$$z^a = x_0 y_0 + \sum_{i=1}^{n} (x_0 y_i + x_i y_0)\varepsilon_i. \tag{50}$$

The real and imaginary approximation error partial deviations, z_{real} and z_{imag}, are similar and given by (cf. equation (35) for the real affine multiplication)

$$\begin{aligned} z_{\text{real}} = {} & |\text{Re}(x_0)| y_{\text{real}} + x_{\text{real}} |\text{Re}(y_0)| + |\text{Im}(x_0)| y_{\text{imag}} + x_{\text{imag}} |\text{Im}(y_0)| \\ & + \left[\left(\sum_{i=1}^{n} |\text{Re}(x_i)| + x_{\text{real}} \right) \times \left(\sum_{i=1}^{n} |\text{Re}(y_i)| + y_{\text{real}} \right) \right] \\ & + \left[\left(\sum_{i=1}^{n} |\text{Im}(x_i)| + x_{\text{imag}} \right) \times \left(\sum_{i=1}^{n} |\text{Im}(y_i)| + y_{\text{imag}} \right) \right] \end{aligned} \tag{51}$$

and

$$\begin{aligned} z_{\text{imag}} = {} & |\text{Im}(x_0)| y_{\text{real}} + x_{\text{real}} |\text{Im}(y_0)| + |\text{Re}(x_0)| y_{\text{imag}} + x_{\text{imag}} |\text{Re}(y_0)| \\ & + \left[\left(\sum_{i=1}^{n} |\text{Re}(x_i)| + x_{\text{real}} \right) \times \left(\sum_{i=1}^{n} |\text{Im}(y_i)| + y_{\text{imag}} \right) \right] \\ & + \left[\left(\sum_{i=1}^{n} |\text{Im}(x_i)| + x_{\text{imag}} \right) \times \left(\sum_{i=1}^{n} |\text{Re}(y_i)| + y_{\text{real}} \right) \right]. \end{aligned} \tag{52}$$

It is the author's opinion that, in the vast majority of cases, the above simplistic approximation would result in a large overestimation of the true range. The extension from the real to the complex plane has introduced an extra dimension whereby careful 'book-keeping' will result in significantly tighter bounds. The expression for the affine approximation, z^a, is the same as Eq. (36) with the only difference being that the coefficients, x_0, y_0, x_i and y_i, will be complex in this case

$$z^a = \left(x_0 y_0 + \frac{1}{2} \sum_{i=1}^{n} x_i y_i \right) + \sum_{i=1}^{n} (x_0 y_i + x_i y_0)\varepsilon_i. \tag{53}$$

The real and imaginary approximation error partial deviations, z_{real} and z_{imag}, are given by (cf. Eq. (37) for the real affine multiplication)

$$\begin{aligned} z_{\text{real}} = {} & \frac{1}{2} \sum_{i=1}^{n} |\text{Re}(x_i y_i)| + \sum_{i=1}^{n} \sum_{j=i+1}^{n} |\text{Re}(x_i y_j + x_j y_i)| + x_{\text{real}} y_{\text{real}} + x_{\text{imag}} y_{\text{imag}} \\ & + \left[\left(|\text{Re}(x_0)| + \sum_{i=1}^{n} |\text{Re}(x_i)| \right) \times y_{\text{real}} \right] + \left[\left(|\text{Im}(x_0)| + \sum_{i=1}^{n} |\text{Im}(x_i)| \right) \times y_{\text{imag}} \right] \\ & + \left[x_{\text{real}} \times \left(|\text{Re}(y_0)| + \sum_{i=1}^{n} |\text{Re}(y_i)| \right) \right] + \left[x_{\text{imag}} \times \left(|\text{Im}(y_0)| + \sum_{i=1}^{n} |\text{Im}(y_i)| \right) \right] \end{aligned} \tag{54}$$

and

$$z_{\text{imag}} = \frac{1}{2}\sum_{i=1}^{n}|\text{Im}(x_i y_i)| + \sum_{i=1}^{n}\sum_{j=i+1}^{n}|\text{Im}(x_i y_j + x_j y_i)| + x_{\text{real}}y_{\text{imag}} + x_{\text{imag}}y_{\text{real}} + \left[\left(|\text{Re}(x_0)| + \sum_{i=1}^{n}|\text{Re}(x_i)|\right) \times y_{\text{imag}}\right] + \left[\left(|\text{Im}(x_0)| + \sum_{i=1}^{n}|\text{Im}(x_i)|\right) \times y_{\text{real}}\right] + \left[x_{\text{real}} \times \left(|\text{Im}(y_0)| + \sum_{i=1}^{n}|\text{Im}(y_i)|\right)\right] + \left[x_{\text{imag}} \times \left(|\text{Re}(y_0)| + \sum_{i=1}^{n}|\text{Re}(y_i)|\right)\right]. \quad (55)$$

The expressions for z^a, z_{real} and z_{imag} may appear to be complicated but they are simply an extension of the expressions given in Eqs. (36) and (37) for the real case.

It is slightly difficult to compare the complex affine arithmetic multiplication with its complex interval arithmetic counterpart discussed in Section 3. The reason for this is that the amount of dependency within and between the two operands has a significant bearing on the resulting affine solution whilst it has no bearing on the resulting interval solution. In order to illustrate this point, the numerical examples of Section 3 will be revisited. Fig. 1 showed the solution set (assuming independence of all four operand components) of the multiplication of $([3,7] + \text{i}[2,4])$ by $([9,11] - \text{i}([2,4])$ and the box calculated using complex interval arithmetic. Three cases will now be considered.

5.1. Multiplication example 1: all four real and imaginary components independent

First, let $\hat{x} = (5 + 3\text{i}) + 2\varepsilon_1 - \text{i}\varepsilon_2$ and $\hat{y} = (10 - 3\text{i}) + \varepsilon_3 + \text{i}\varepsilon_4$. Conversion of $\hat{x}$ and $\hat{y}$ to complex intervals using Eq. (42) give the same values as used in the complex interval examples. Also, note that there is no dependency between the real and imaginary components of $\hat{x}$ or $\hat{y}$. Therefore, the operands have the same level of independence as their interval counterparts. Using Eqs. (50)–(52) gives $\hat{z}$, the affine approximation of the multiplication of $\hat{x}$ and $\hat{y}$, as

$$\hat{z} = (59 + 15\text{i}) + (20 - 6\text{i})\varepsilon_1 + (-3 - 10\text{i})\varepsilon_2 + (5 + 3\text{i})\varepsilon_3 + (-3 + 5\text{i})\varepsilon_4 + 3\varepsilon_{\text{real}_z} + 3\text{i}\varepsilon_{\text{imag}_z}. \quad (56)$$

The convex hull given by the above equation is shown as a solid line in Fig. 4 whilst the dotted box is the complex interval calculated in Section 3 and the dashed line contains the true solution set for the multiplication of the two terms with independent real and imaginary components. Although complex interval arithmetic returns the smallest box which contains the solution set, the complex convex hull returned by complex affine arithmetic gives a better idea of the relationship between the real and imaginary components of the solution.

5.2. Multiplication example 2: dependency between real and imaginary components within both operands

The real advantage of complex affine arithmetic over complex interval arithmetic becomes more apparent in the second example where the partial deviations are complex as opposed to real *or* imaginary as in the last example. So, let $\hat{x} = (5 + 3\text{i}) + (2 - \text{i})\varepsilon_1$ and $\hat{y} = (10 - 3\text{i}) + (1 + \text{i})\varepsilon_2$. Again, these affine forms convert to the same complex intervals as previously. On this occasion,

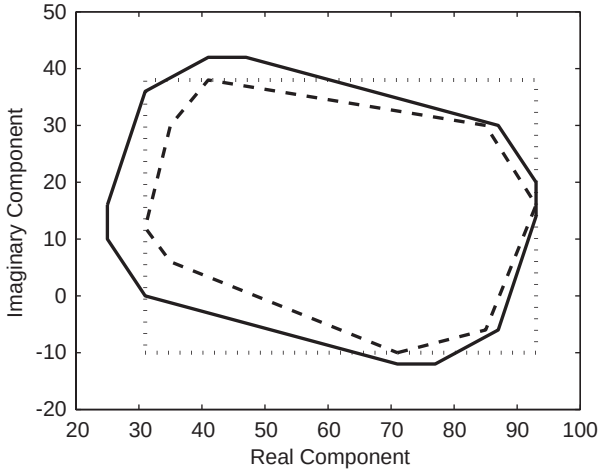

Fig. 4. Complex affine multiplication of $(5+3\mathrm{i})+2\varepsilon_1-\mathrm{i}\varepsilon_2$ and $(10-3\mathrm{i})+\varepsilon_3+\mathrm{i}\varepsilon_4$ shown as solid hull. True solution set boundary shown as dashed line and complex interval box as dotted line.

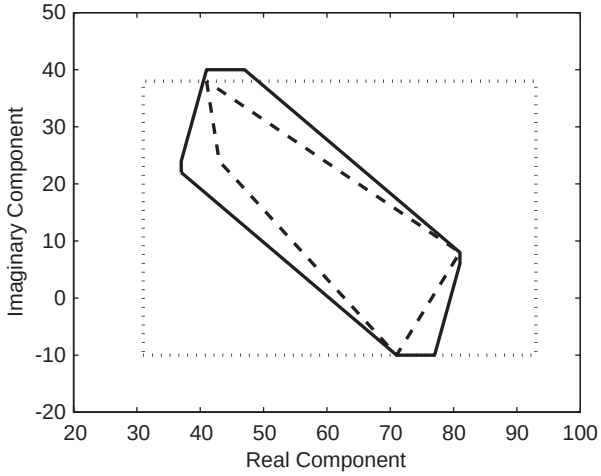

Fig. 5. Complex affine multiplication of $(5+3\mathrm{i})+(2-\mathrm{i})\varepsilon_1$ and $(10-3\mathrm{i})+(1+\mathrm{i})\varepsilon_2$ shown as solid hull. True solution set boundary shown as dashed line and complex interval box as dotted line.

however, dependency exists between the real and imaginary components of each form, although there is no dependency *between* the two forms. Using Eqs. (50) to (52) gives $\hat{z}$, the affine approximation of the multiplication of $\hat{x}$ and $\hat{y}$, as

$$\hat{z} = (59+15\mathrm{i})+(17-16\mathrm{i})\varepsilon_1+(2+8\mathrm{i})\varepsilon_2+3\varepsilon_{\mathrm{real}_z}+\mathrm{i}\varepsilon_{\mathrm{imag}_z}. \tag{57}$$

The convex hull given by the above equation is shown as a solid line in Fig. 5 whilst the dotted box is again the complex interval. The dashed line contains the true solution set for the multiplication

of the two terms with dependent real and imaginary components. The advantage of complex affine arithmetic starts to become more apparent in this example with the convex hull giving a significantly closer fit to the true solution set than that returned by complex interval arithmetic.

5.3. Multiplication example 3: dependency between all four real and imaginary components

The final example considers the case when the partial deviations of the two affine forms are complex and there exists a relationship between the two forms. Let $\hat{x} = (5 + 3\mathrm{i}) + (2 - \mathrm{i})\varepsilon_1$ and $\hat{y} = (10 - 3\mathrm{i}) + (1 + \mathrm{i})\varepsilon_1$ (as before but with ε_2 substituted with ε_1). Using Eqs. (50)–(52) gives $\hat{z}$, the affine approximation of the multiplication of $\hat{x}$ and $\hat{y}$, as

$$\hat{z} = (60.5 + 15.5\mathrm{i}) + (19 - 8\mathrm{i})\varepsilon_1 + 1.5\varepsilon_{\mathrm{real}_z} + 0.5\mathrm{i}\varepsilon_{\mathrm{imag}_z}. \tag{58}$$

The true solution set on this occasion is simply the dashed curved line shown in Fig. 6. This is closely bounded by the solid-lined convex hull given by Eq. (58). Due to its inability to deal with the relationships between and within the operands, complex interval arithmetic returns the same bounds as for the previous cases.

The final basic operation to be considered for complex affine forms is division of one form by another. This operation may not be represented by an affine combination of the ε_i. The way that this operation will be considered is the multiplication of the product of the numerator and the complex conjugate of the denominator by the reciprocal of the product of the denominator and its complex conjugate. This may be written

$$\begin{aligned}\frac{\hat{x}}{\hat{y}} &= \frac{\mathrm{Re}(\hat{x}) + \mathrm{iIm}(\hat{x})}{\mathrm{Re}(\hat{y}) + \mathrm{iIm}(\hat{y})} = \frac{(\mathrm{Re}(\hat{x}) + \mathrm{iIm}(\hat{x}))(\mathrm{Re}(\hat{y}) - \mathrm{iIm}(\hat{y}))}{\mathrm{Re}(\hat{y})^2 + \mathrm{Im}(\hat{y})^2} \\ &= (\mathrm{Re}(\hat{x}) + \mathrm{iIm}(\hat{x}))(\mathrm{Re}(\hat{y}) - \mathrm{iIm}(\hat{y})) \times \frac{1}{\mathrm{Re}(\hat{y})^2 + \mathrm{Im}(\hat{y})^2}.\end{aligned} \tag{59}$$

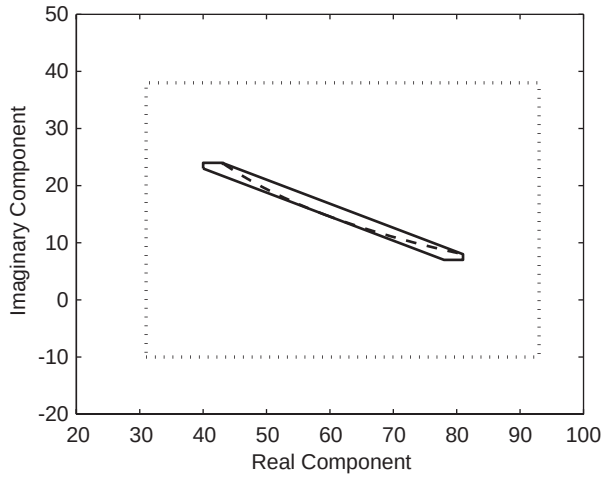

Fig. 6. Complex affine multiplication of $(5 + 3\mathrm{i}) + (2 - \mathrm{i})\varepsilon_1$ and $(10 - 3\mathrm{i}) + (1 + \mathrm{i})\varepsilon_1$ shown as solid hull. True solution set boundary shown as dashed line and complex interval box as dotted line.

It should be noted that, if a complex affine multiplication of the denominator and its complex conjugate were calculated using Eqs. (50)–(52), the product would have a non-zero imaginary component. It is for this reason that the product is forced to be the sum of the real part of the denominator squared and the imaginary part squared thereby ensuring a purely real term. The reciprocal and squared functions will be calculated using the Chebyshev approximations given in Eqs. (38)–(40).

In the same way as the power of complex affine multiplication was illustrated, so the same three examples will be used to show the effect of adopting a complex affine approach to division over a complex interval one.

5.4. Division example 1: all four real and imaginary components independent

The complex affine forms for the first case are the same as those used in the multiplication first case, i.e. $\hat{x} = (5 + 3\mathrm{i}) + 2\varepsilon_1 - \mathrm{i}\varepsilon_2$ and $\hat{y} = (10 - 3\mathrm{i}) + \varepsilon_3 + \mathrm{i}\varepsilon_4$. So there is no dependency between the real and imaginary components of $\hat{x}$ or $\hat{y}$ and the operands have the same level of independence as their interval counterparts used in the complex interval division example of Section 3 shown in Fig. 2. Using the approach detailed above gives $\hat{z}$, the affine approximation of the division of $\hat{x}$ by $\hat{y}$, as

$$\begin{aligned}\hat{z} = {} & (0.3809 + 0.4180\mathrm{i}) + (0.1858 + 0.0557\mathrm{i})\varepsilon_1 + (0.0279 - 0.0929\mathrm{i})\varepsilon_2 \\ & + (-0.0252 - 0.0510\mathrm{i})\varepsilon_3 + (0.0498 - 0.0231\mathrm{i})\varepsilon_4 + 0.0937\varepsilon_{\mathrm{real}_z} + 0.0871\mathrm{i}\varepsilon_{\mathrm{imag}_z}. \end{aligned} \quad (60)$$

This is shown in Fig. 7 as the solid convex hull. As with the multiplication, although there is no significant improvement in terms of the area within the hull when compared to the interval box, the complex affine hull conveys to some extent the relationship between the real and imaginary parts of the solution set which is illustrated as a dashed line.

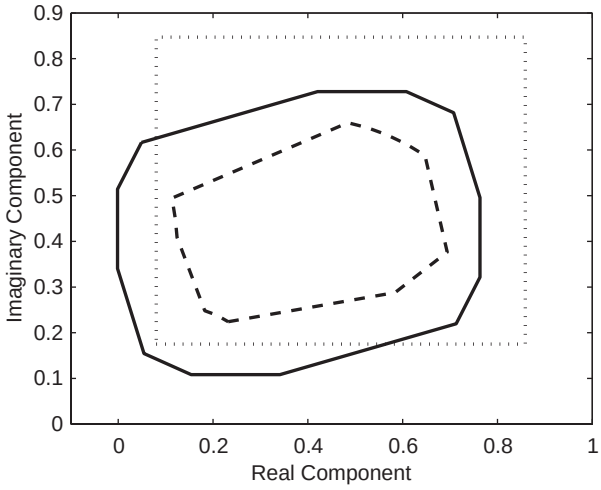

Fig. 7. Complex affine division of $(5 + 3\mathrm{i}) + 2\varepsilon_1 - \mathrm{i}\varepsilon_2$ by $(10 - 3\mathrm{i}) + \varepsilon_3 + \mathrm{i}\varepsilon_4$ shown as solid hull. True solution set boundary shown as dashed line and complex interval box as dotted line.

5.5. Division example 2: dependency between real and imaginary components within both operands

The second example considers the effect of dividing $\hat{x} = (5 + 3\mathrm{i}) + (2 - \mathrm{i})\varepsilon_1$ by $\hat{y} = (10 - 3\mathrm{i}) + (1 + \mathrm{i})\varepsilon_2$. Using Eqs. (50)–(52) and (38)–(40) gives $\hat{z}$, the affine approximation of the division of $\hat{x}$ and $\hat{y}$, as

$$\hat{z} = (0.3715 + 0.4141\mathrm{i}) + (0.2105 - 0.0349\mathrm{i})\varepsilon_1 + (0.0251 - 0.0714\mathrm{i})\varepsilon_2 + 0.0403\varepsilon_{\mathrm{real}_z} + 0.0416\mathrm{i}\varepsilon_{\mathrm{imag}_z}. \tag{61}$$

The convex hull given by the above equation is shown as a solid line in Fig. 8 giving a much better approximation to the true solution set (dashed line) than that offered by complex interval arithmetic (dotted box).

5.6. Division example 3: dependency between all four real and imaginary components

Finally, let $\hat{x} = (5 + 3\mathrm{i}) + (2 - \mathrm{i})\varepsilon_1$ and $\hat{y} = (10 - 3\mathrm{i}) + (1 + \mathrm{i})\varepsilon_1$. $\hat{z}$, the affine approximation of the division of $\hat{x}$ and $\hat{y}$, is now

$$\hat{z} = (0.3626 + 0.4027\mathrm{i}) + (0.2355 - 0.1063\mathrm{i})\varepsilon_1 + 0.0313\varepsilon_{\mathrm{real}_z} + 0.0302\mathrm{i}\varepsilon_{\mathrm{imag}_z}. \tag{62}$$

The true solution set is the dashed curved line shown in Fig. 9 which may be seen to be reasonably closely bounded by the convex hull, shown as solid line. Again, the complex interval arithmetic is shown as a dotted box.

Now that the arithmetic operations required to perform complex affine arithmetic have been defined and illustrated, a simple academic example will follow in the next section to illustrate the possibilities of this new framework.

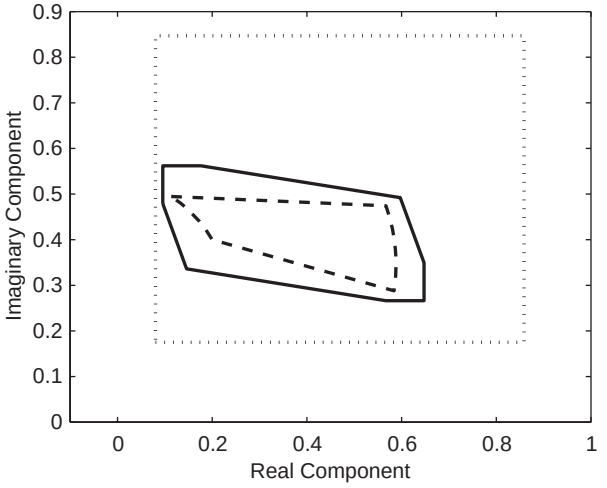

Fig. 8. Complex affine division of $(5 + 3\mathrm{i}) + (2 - \mathrm{i})\varepsilon_1$ by $(10 - 3\mathrm{i}) + (1 + \mathrm{i})\varepsilon_2$ shown as solid hull. True solution set boundary shown as dashed line and complex interval box as dotted line.

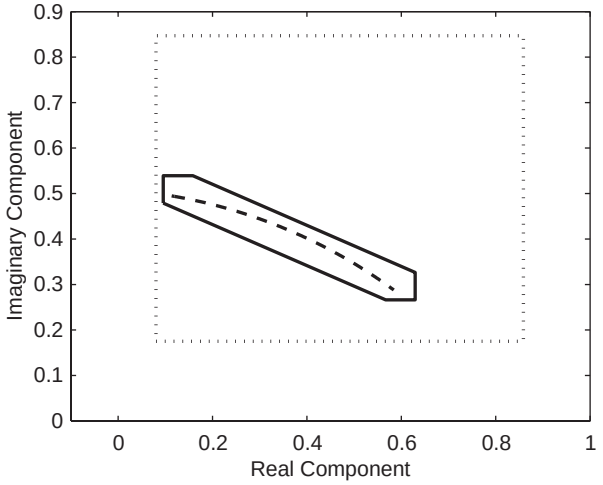

Fig. 9. Complex affine division of $(5+3\mathrm{i})+(2-\mathrm{i})\varepsilon_1$ by $(10-3\mathrm{i})+(1+\mathrm{i})\varepsilon_1$ shown as solid hull. True solution set boundary shown as dashed line and complex interval box as dotted line.

6. Frequency response functions for a two-degree-of-freedom system with uncertain parameters

The problem to be considered here is a two-degree-of-freedom (2dof) lumped mass system as shown in Fig. 10. The masses are denoted by m_1 and m_2, the stiffnesses by k_1, k_2 and k_3 and the viscous dampers by c_1, c_2 and c_3. The simplicity of the system should serve to make the subsequent analysis more transparent whilst allowing straightforward visualisation of the eigenvalues. A discussion of how this method may be extended to more complicated systems and limitations of the approach will be given towards the end of this section.

The equations of motion of the system under forced vibration may be written,

$$M\ddot{Y} + C\dot{Y} + KY = X, \tag{63}$$

where

$$Y = \begin{Bmatrix} y_1 \\ y_2 \end{Bmatrix} \quad \text{and} \quad X = \begin{Bmatrix} x_1 \\ x_2 \end{Bmatrix} \tag{64}$$

with y_1 and y_2 being the displacements of masses m_1 and m_2 respectively and x_1 and x_2 the forcing at the masses. The mass matrix, M, damping matrix, C, and stiffness matrix, K, for the system are given by

$$M = \begin{bmatrix} m_1 & 0 \\ 0 & m_2 \end{bmatrix}, \quad C = \begin{bmatrix} c_1 + c_2 & -c_2 \\ -c_2 & c_2 + c_3 \end{bmatrix} \quad \text{and} \quad K = \begin{bmatrix} k_1 + k_2 & -k_2 \\ -k_2 & k_2 + k_3 \end{bmatrix}. \tag{65}$$

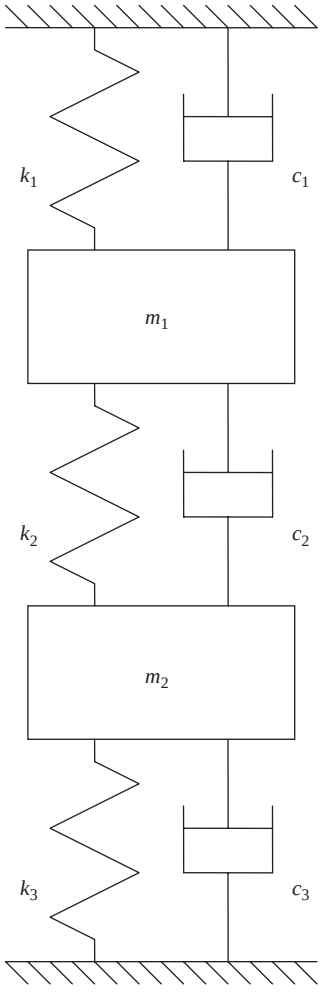

Fig. 10. Two-degree-of-freedom lumped mass system.

The frequency response functions (FRFs) of the system relate the response at some point j to a force input at some point i and they may be obtained by probing the system with harmonic excitations for x_1 and x_2. The resulting FRF matrix for this system is found to be

$$\begin{bmatrix} H_{11}(\omega) & H_{12}(\omega) \\ H_{21}(\omega) & H_{22}(\omega) \end{bmatrix} = \begin{bmatrix} (k_1+k_2)+\mathrm{i}\omega(c_1+c_2)-m_1\omega^2 & -k_2-\mathrm{i}\omega c_2 \\ -k_2-\mathrm{i}\omega c_2 & (k_2+k_3)+\mathrm{i}\omega(c_2+c_3)-m_2\omega^2 \end{bmatrix}^{-1}, \quad (66)$$

where $H_{ij}(\omega)$ is the FRF for a response at point j to an input at point i and ω is the frequency of vibration. The above equation may be written

$$\begin{bmatrix} H_{11}(\omega) & H_{12}(\omega) \\ H_{21}(\omega) & H_{22}(\omega) \end{bmatrix} = \frac{1}{D(\omega)} \begin{bmatrix} (k_2+k_3)+\mathrm{i}\omega(c_2+c_3)-m_2\omega^2 & k_2+\mathrm{i}\omega c_2 \\ k_2+\mathrm{i}\omega c_2 & (k_1+k_2)+\mathrm{i}\omega(c_1+c_2)-m_1\omega^2 \end{bmatrix}, \tag{67}$$

where $D(\omega)$ is the determinant of the matrix on the right-hand side of Eq. (66) given by

$$D(\omega) = ((k_1+k_2)+\mathrm{i}\omega(c_1+c_2)-m_1\omega^2)((k_2+k_3)+\mathrm{i}\omega(c_2+c_3)-m_2\omega^2) - (k_2+\mathrm{i}\omega c_2)^2. \tag{68}$$

Examination of Eq. (67) shows that each frequency line of each of the four FRFs is simply one complex number divided by another. It may also noted that $H_{12}(\omega) = H_{21}(\omega)$ as expected from reciprocity.

6.1. Crisp system

A numerical example will now be considered. The system will be that shown in Fig. 10 with the 'crisp' system (i.e. no uncertain parameters) having parameter values as follows: $m_1 = 1\,\mathrm{kg}$, $m_2 = 2\,\mathrm{kg}$, $c_1 = 10\,\mathrm{Ns/m}$, $c_2 = 20\,\mathrm{Ns/m}$, $c_3 = 30\,\mathrm{Ns/m}$, $k_1 = 10^4\,\mathrm{N/m}$, $k_2 = 2\times10^4\,\mathrm{N/m}$ and $k_3 = 3\times10^4\,\mathrm{N/m}$. Substituting these values into Eq. (66) yields the four FRFs for the system. Fig. 11 shows $H_{11}(\omega)$ for the crisp system in terms of amplitude and phase plotted between 0 and 400 rad/s in steps of 0.25 rad/s (this frequency range and step will also be used in the following analyses). From this point, the FRFs will be presented in terms of real and imaginary components as it is in this format that it was decided was best for calculation once uncertainty was introduced. Conversion of the uncertain FRFs to amplitude and phase would clearly be possible although it is not considered here.

Performing an eigenvalue analysis of the undamped version of this crisp system results in eigenvalues equal to $1.3139\times10^4\,(\mathrm{rad/s})^2$ and $4.1861\times10^4\,(\mathrm{rad/s})^2$ which translate into undamped natural frequencies of 114.6 and 204.6 rad/s.

6.2. Random scanning from bounded ranges

The question which will now be addressed is what happens to the FRFs when uncertainty is introduced into the parameters. Each of the eight structural parameters were assumed uncertain but lying within a range of $\pm1\%$ of their corresponding crisp values.

In order to get a benchmark for the effect of this uncertainty upon the FRFs, a benchmark simulation was conducted. This consisted running the 'crisp' calculation 5000 times but with the values of the parameters randomly drawn from the specified ranges. Uniform distributions were assumed for all ranges in order to have better assessment of the extreme events than would be likely with Gaussian-type distributions. It should be stated that the number of simulations was

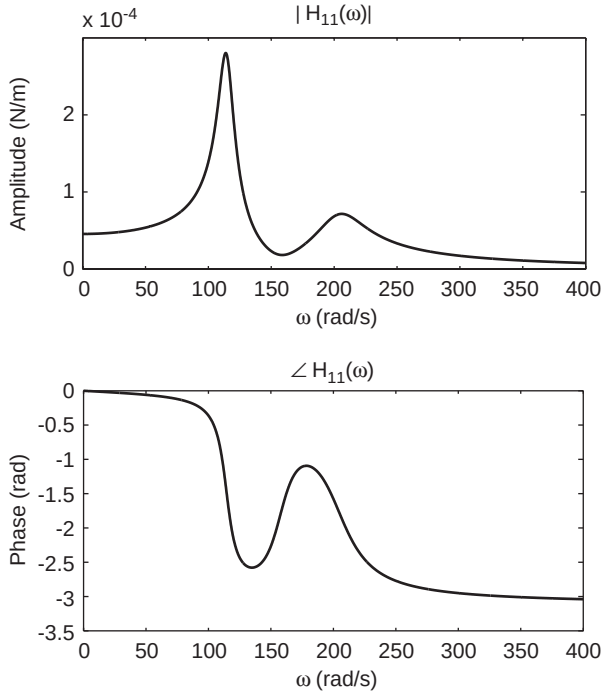

Fig. 11. Magnitude and phase of $H_{11}(\omega)$.

chosen rather arbitrarily: the desire was to have *adequate* coverage of the input parameter space within a *reasonable* computation time. Towards the end of this section, a further simulation will be conducted using a number of simulations which require a similar amount of computation time as the complex affine analysis calculation. This should allow better comparison of the two methods.

The frequency regions which showed the most interesting behaviour were around the two natural frequencies of the system and therefore were the areas plotted in the following figures. Figs. 12–17 show the effect of uncertainty upon the real and imaginary components of the three distinct FRFs in the frequency ranges 90–140 and 180–230 rad/s. The crisp FRFs are shown as solid lines whilst the lower and upper bounds returned by the random scanning simulation are shown as dotted lines.

6.3. Interval analysis

Analysing the system using complex interval arithmetic is simply a matter of considering intervalised versions of Eqs. (66) and (67). The equations for the three distinct interval FRFs (as $\mathbf{H}_{21}(\omega) = \mathbf{H}_{12}(\omega)$) are

$$\mathbf{H}_{11}(\omega) = \frac{(\mathbf{k}_2 + \mathbf{k}_3) + \mathrm{i}\omega(\mathbf{c}_2 + \mathbf{c}_3) - \mathbf{m}_2\omega^2}{((\mathbf{k}_1 + \mathbf{k}_2) + \mathrm{i}\omega(\mathbf{c}_1 + \mathbf{c}_2) - \mathbf{m}_1\omega^2)((\mathbf{k}_2 + \mathbf{k}_3) + \mathrm{i}\omega(\mathbf{c}_2 + \mathbf{c}_3) - \mathbf{m}_2\omega^2) - (\mathbf{k}_2 + \mathrm{i}\omega\mathbf{c}_2)^2}, \quad (69)$$

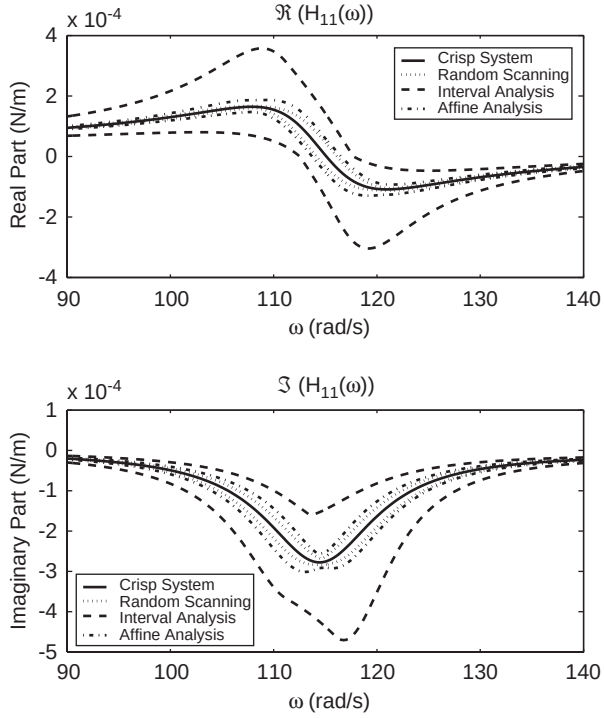

Fig. 12. Real and imaginary components of $H_{11}(\omega)$ in frequency range 90–140 rad/s.

$$\mathbf{H}_{12}(\omega) = \frac{\mathbf{k}_2 + \mathrm{i}\omega\mathbf{c}_2}{((\mathbf{k}_1 + \mathbf{k}_2) + \mathrm{i}\omega(\mathbf{c}_1 + \mathbf{c}_2) - \mathbf{m}_1\omega^2)((\mathbf{k}_2 + \mathbf{k}_3) + \mathrm{i}\omega(\mathbf{c}_2 + \mathbf{c}_3) - \mathbf{m}_2\omega^2) - (\mathbf{k}_2 + \mathrm{i}\omega\mathbf{c}_2)^2}, \quad (70)$$

$$\mathbf{H}_{22}(\omega) = \frac{(\mathbf{k}_1 + \mathbf{k}_2) + \mathrm{i}\omega(\mathbf{c}_1 + \mathbf{c}_2) - \mathbf{m}_1\omega^2}{((\mathbf{k}_1 + \mathbf{k}_2) + \mathrm{i}\omega(\mathbf{c}_1 + \mathbf{c}_2) - \mathbf{m}_1\omega^2)((\mathbf{k}_2 + \mathbf{k}_3) + \mathrm{i}\omega(\mathbf{c}_2 + \mathbf{c}_3) - \mathbf{m}_2\omega^2) - (\mathbf{k}_2 + \mathrm{i}\omega\mathbf{c}_2)^2}. \quad (71)$$

Each of the parameters are written as a range given by the crisp value ±1% of this value. This gives the parameter ranges

$$\mathbf{m}_1 = [0.99, 1.01], \quad \mathbf{m}_2 = [1.98, 2.02], \quad \mathbf{c}_1 = [9.9, 10.1], \quad \mathbf{c}_2 = [19.8, 20.2], \quad \mathbf{c}_3 = [29.7, 30.3]$$
$$\mathbf{k}_1 = [0.99 \times 10^4, 1.01 \times 10^4], \quad \mathbf{k}_2 = [1.98 \times 10^4, 2.02 \times 10^4], \quad \mathbf{k}_3 = [2.97 \times 10^4, 3.03 \times 10^4] \quad (72)$$

which are substituted into the above equations and solved using the complex interval arithmetic operations of Eqs. (19)–(23) for each value of ω. The resulting lower and upper bounds of the interval FRFs are shown in Figs. 12–17 as dashed lines.

6.4. *Affine analysis*

Analysis of the system using complex affine arithmetic is conducted in much the same manner as for interval analysis. The equations for the three distinct affine FRFs are the same as

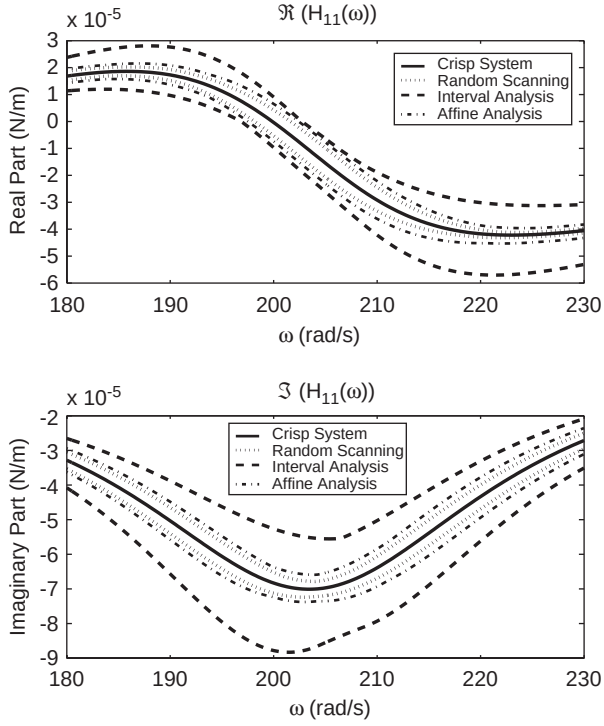

Fig. 13. Real and imaginary components of $H_{11}(\omega)$ in frequency range 180–230 rad/s.

Eqs. (69)–(71) with all interval ranges being replaced with affine forms

$$\hat{H}_{11}(\omega) = \frac{(\hat{k}_2 + \hat{k}_3) + \mathrm{i}\omega(\hat{c}_2 + \hat{c}_3) - \hat{m}_2\omega^2}{((\hat{k}_1 + \hat{k}_2) + \mathrm{i}\omega(\hat{c}_1 + \hat{c}_2) - \hat{m}_1\omega^2)((\hat{k}_2 + \hat{k}_3) + \mathrm{i}\omega(\hat{c}_2 + \hat{c}_3) - \hat{m}_2\omega^2) - (\hat{k}_2 + \mathrm{i}\omega\hat{c}_2)^2}, \quad (73)$$

$$\hat{H}_{12}(\omega) = \frac{\hat{k}_2 + \mathrm{i}\omega\hat{c}_2}{((\hat{k}_1 + \hat{k}_2) + \mathrm{i}\omega(\hat{c}_1 + \hat{c}_2) - \hat{m}_1\omega^2)((\hat{k}_2 + \hat{k}_3) + \mathrm{i}\omega(\hat{c}_2 + \hat{c}_3) - \hat{m}_2\omega^2) - (\hat{k}_2 + \mathrm{i}\omega\hat{c}_2)^2}, \quad (74)$$

$$\hat{H}_{22}(\omega) = \frac{(\hat{k}_1 + \hat{k}_2) + \mathrm{i}\omega(\hat{c}_1 + \hat{c}_2) - \hat{m}_1\omega^2}{((\hat{k}_1 + \hat{k}_2) + \mathrm{i}\omega(\hat{c}_1 + \hat{c}_2) - \hat{m}_1\omega^2)((\hat{k}_2 + \hat{k}_3) + \mathrm{i}\omega(\hat{c}_2 + \hat{c}_3) - \hat{m}_2\omega^2) - (\hat{k}_2 + \mathrm{i}\omega\hat{c}_2)^2}. \quad (75)$$

In affine form, each of the parameters is written as a central value (equal to the crisp value) plus a partial deviation term (equal to 1% of the crisp value). This gives the following parameter affine forms:

$$\hat{m}_1 = 1 + 0.01\varepsilon_{m_1}, \quad \hat{m}_2 = 2 + 0.02\varepsilon_{m_2}, \quad \hat{c}_1 = 10 + 0.1\varepsilon_{c_1}, \quad \hat{c}_2 = 20 + 0.2\varepsilon_{c_2}, \quad \hat{c}_3 = 30 + 0.3\varepsilon_{c_3},$$
$$\hat{k}_1 = 10^4 + 10^2\varepsilon_{k_1}, \quad \hat{k}_2 = (2 \times 10^4) + (2 \times 10^2)\varepsilon_{k_2}, \quad \hat{k}_3 = (3 \times 10^4) + (3 \times 10^2)\varepsilon_{k_3}. \quad (76)$$

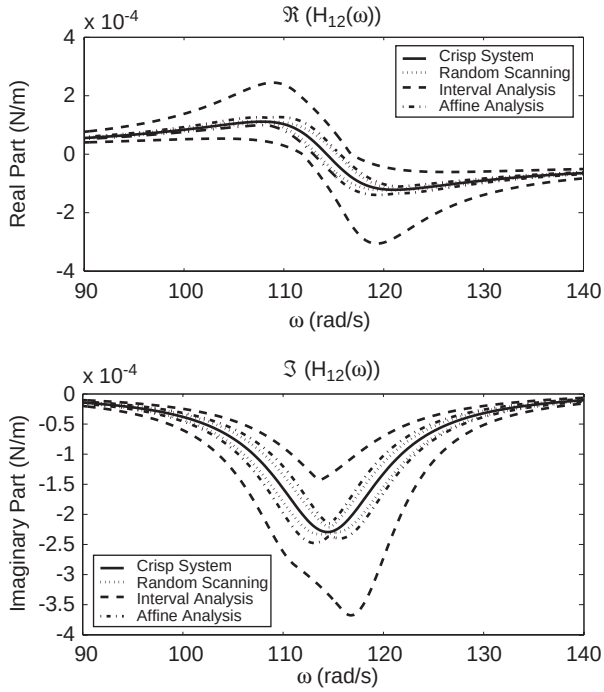

Fig. 14. Real and imaginary components of $H_{12}(\omega)$ in frequency range 90–140 rad/s.

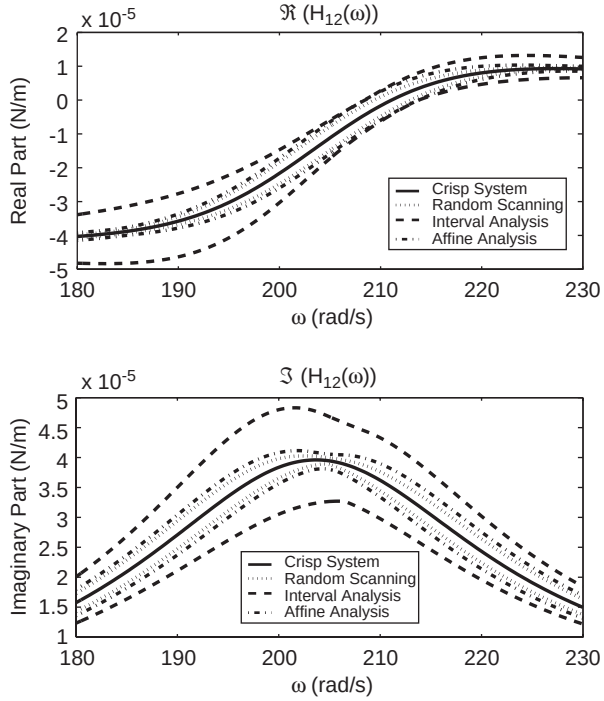

Fig. 15. Real and imaginary components of $H_{12}(\omega)$ in frequency range 180–230 rad/s.

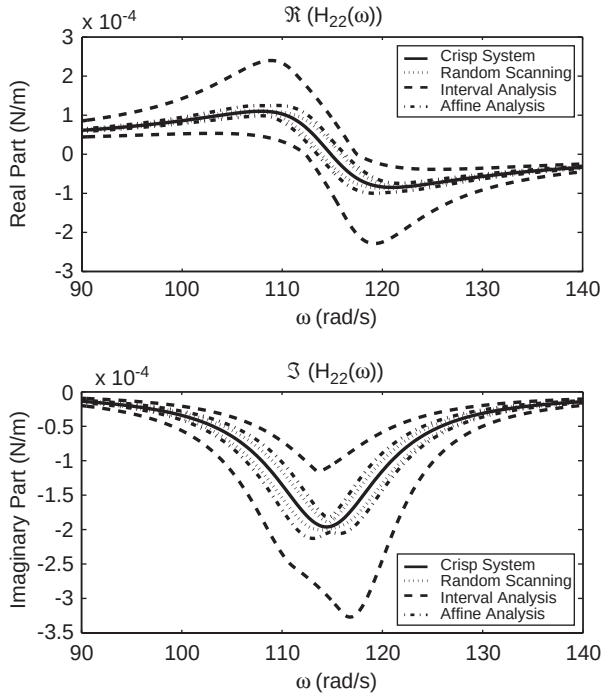

Fig. 16. Real and imaginary components of $H_{22}(\omega)$ in frequency range 90–140 rad/s.

These affine forms are substituted into the above equations which are then solved using the complex affine arithmetic expressions given in Eqs. (45)–(49), (53)–(55) and (59) (and Eqs. (38)–(40) from the real affine analysis section). The resulting bounds of the affine FRFs are shown in Figs. 12–17 as dot-dashed lines.

6.5. Comparison of results

Examination of the Figs. 12–17 highlights several points. Firstly, the real and imaginary components of $H_{11}(\omega)$, $H_{12}(\omega)$ and $H_{22}(\omega)$ in the 90–140 rad/s range show similar trends. This is the case for crisp, random scanning, interval and affine analyses.

The next point worth noting is that, in all the plots, the crisp FRF *must* lie within each of the pairs of bounds. It is also the case that the random scanning bounds *must* lie within (or be coincident with) the bounds returned by complex interval and affine analysis. The reason for this is that each random scanning simulation returns an FRF which is guaranteed to be *within* the solution set of all possible FRFs whilst the complex interval and complex affine analyses are conservative and, as such, are guaranteed to return bounds which *contain* the solution set.

The most important point with regards to the purpose of this paper is that, in all the plots in Figs. 12–17, the bounds returned by complex affine arithmetic are significantly narrower than those returned by complex interval arithmetic. Many papers, including two by the author [16,18], have demonstrated the advantages or real affine arithmetic over real interval arithmetic, but these

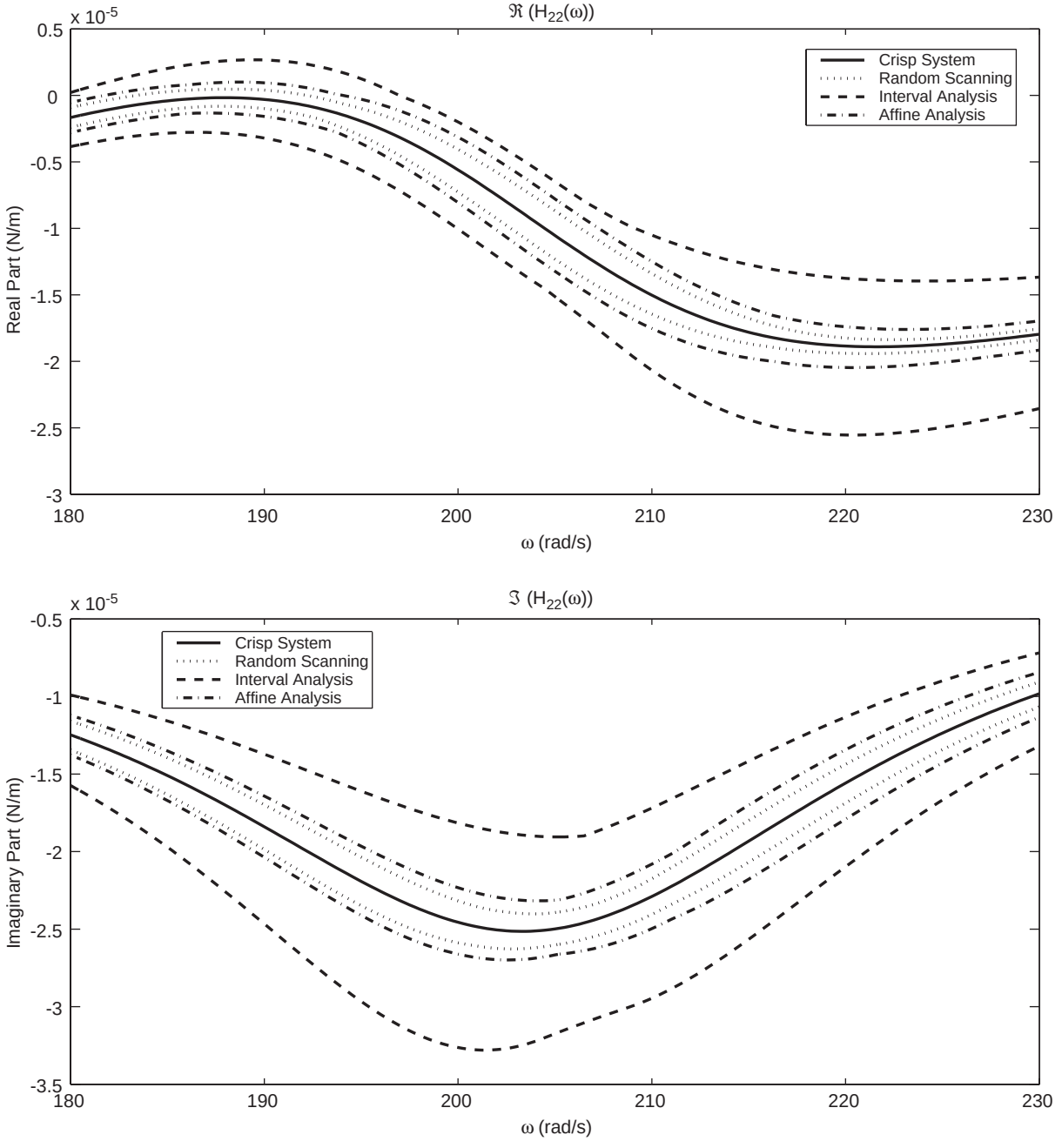

Fig. 17. Real and imaginary components of $H_{22}(\omega)$ in frequency range 180–230 rad/s.

preliminary results appear to show that there is an even greater potential for improvement upon complex interval arithmetic offered by this newly developed complex affine arithmetic. The reason for these benefits is the very same reason for the improvement in the complex affine analysis

examples in Section 5 over the complex interval analysis approach in Section 3, namely the ability of affine analysis to keep track of dependencies between terms (and between the real and imaginary components of terms) thus reducing overestimation. It should also be stated that, if the analysis is taken one step further to calculate amplitude and phase envelopes of the FRFs, the dependency tracking between real and imaginary components offered by complex affine analysis will result in less conservative conversion than that which would result using complex interval analysis.

The results returned by complex affine arithmetic in all the plots are reasonably tight to the random scanning bounds, but these results must be put into context with respect to computational time and, before drawing any general conclusions, with respect to the particular situation.

In the majority of situations it is not feasible to conduct a vast number of model runs in order to ascertain the effect of input parameter uncertainty on some output parameter. In this example, a single crisp run (calculation of three FRFs with 1600 sample lines) required 0.2 s on a 1.70 GHz, 512 MB RAM laptop with Pentium 4 processor. The completion of 5000 random scanning simulations required 1351 s (22.5 min) whilst the complex interval arithmetic and complex affine arithmetic required 17.5 and 82.8 s, respectively. So the complex affine arithmetic requires almost five times the computational time as the complex interval arithmetic but this is easily justified by the results. As stated previously, the choice of 5000 simulations for the random scanning approach was rather arbitrary. A *fairer* comparison, in terms of computation time, of the random scanning and complex affine analysis approaches is afforded shortly during the discussion of the inner and outer bounds returned by affine analysis.

In many situations, where simply a reasonable approximation of output parameters is required and computational time is not an issue, random scanning predictions will often suffice. However, in safety-critical situations, where knowledge of all possible outcomes is essential, then a technique which returns solutions which are *guaranteed* to contain all possible outcomes is clearly desirable: this argument holds even if the computational model takes a relatively short time to run. It should be made very clear that, as the number of uncertain parameters increases, so the number of random scanning simulations required to return a good approximation of the true solution set grows explosively. The reliance on the results returned by an insufficient number of simulations is potentially disastrous. The other main driver for uncertainty propagation techniques is computational efficiency whereby a single model run (or at least a fraction of the number of runs required by random scanning simulation) returns output parameter information for a *family* of models which lie within the parameter ranges.

6.6. *Affine analysis inner and outer bounds*

Affine arithmetic has two very important advantages over interval arithmetic, aside from the ability to give significantly better bounds in many situations, which are not highlighted often enough. The first of these is the sensitivity information which is returned by affine arithmetic in the form of the partial deviations related to each particular source of uncertainty. It is a simple matter to see which of the input uncertainties have a large bearing on the uncertainty of a particular output parameter; this is not possible with interval arithmetic.

The second advantage over interval arithmetic relates to the fact that it is possible to judge the level of conservatism of the affine analysis due to the inclusion of an approximation error term (or

terms in the case of complex affine analysis). This means that it is possible to return *inner* and *outer* on the lower and upper bounds of the FRFs. Consider, for example, the affine form, $x_0 + \sum_{i=1}^{n} x_i \varepsilon_i + x_{\text{err}} \varepsilon_{\text{err}}$. The outer upper bound is given by $x_0 + \sum_{i=1}^{n} |x_i| + x_{\text{err}}$ whilst the outer lower bound is given by $x_0 - \sum_{i=1}^{n} |x_i| - x_{\text{err}}$. The inner upper bound is given by $x_0 + \sum_{i=1}^{n} |x_i| - x_{\text{err}}$ whilst the inner lower bound is given by $x_0 - \sum_{i=1}^{n} |x_i| + x_{\text{err}}$.

This characteristic is illustrated in Fig. 18 for $H_{11}(\omega)$ in the frequency range 180–190 rad/s. The solid line in both plots represents the crisp FRF whilst the two pairs of dot-dashed lines represent the inner and outer bounds returned by the complex affine arithmetic: the outer bounds are marked with circles and the inner with squares. In order to provide a fairer computational time comparison than previously, 500 random scanning simulations were conducted which took around 80 s (similar to complex affine analysis) on a 1.70 GHz, 512 MB RAM laptop with Pentium 4 processor. In Fig. 18, dotted lines represent the bounds returned by the random scanning simulations. These lines appear to be reasonably coincident with the inner complex affine bounds for both the real and imaginary components. This may initially cause concern at the level of apparent overestimation returned by the outer bounds. This concern proved unfounded when a vertex propagation calculation, comprising 256 (2^8) crisp runs with the 8 input parameters at all possible combinations of their lower and upper bounds, was conducted. The bounds returned by the vertex propagation are represented by dashed lines which must be contained in the solution set and, as such, may be used as an inner bound on the solution set. This approach will rapidly become very inefficient as the number of uncertain parameters increases. Complex affine analysis, however, offers a quick method for calculating inner and outer bounds which are guaranteed to contain the boundaries of the solution set, regardless of the number of uncertain parameters. On a final note, it should be stated that the 500 random scanning simulations significantly underestimate the vertex propagation results, and therefore the true solution set. This situation did not improve significantly when 5000 random scanning simulations were conducted thereby reinforcing concerns expressed earlier about using such an approach in safety-critical situations.

6.7. Extension of method to models of greater complexity

The example included in this section was purposefully simple in order to clearly illustrate the power of complex affine arithmetic when compared to its interval counterpart. That said, the issue of how these ideas may extend to more realistic engineering problems needs to be addressed.

It is the author's opinion that the method would continue to offer significant benefits over interval arithmetic if the system under consideration were a lumped mass system with up to tens of degrees of freedom. In fact, were the system to have a greater number of lumped masses, there would be even greater dependency effects than in the simple example. It is more likely that the number and width of the uncertainty parameters would have a more profound effect on the usefulness of the complex affine approach. As stated previously, tightness of the affine results to the true solution set may be ascertained using inner and outer bounds, or simply by examining the approximation error magnitudes. If the results are not sufficiently tight, the analysis may be repeated with the most influential uncertain parameters (easily identified from partial deviations) being split into several subranges. This will clearly increase computation time but should remain significantly more efficient than the other approaches considered in the paper.

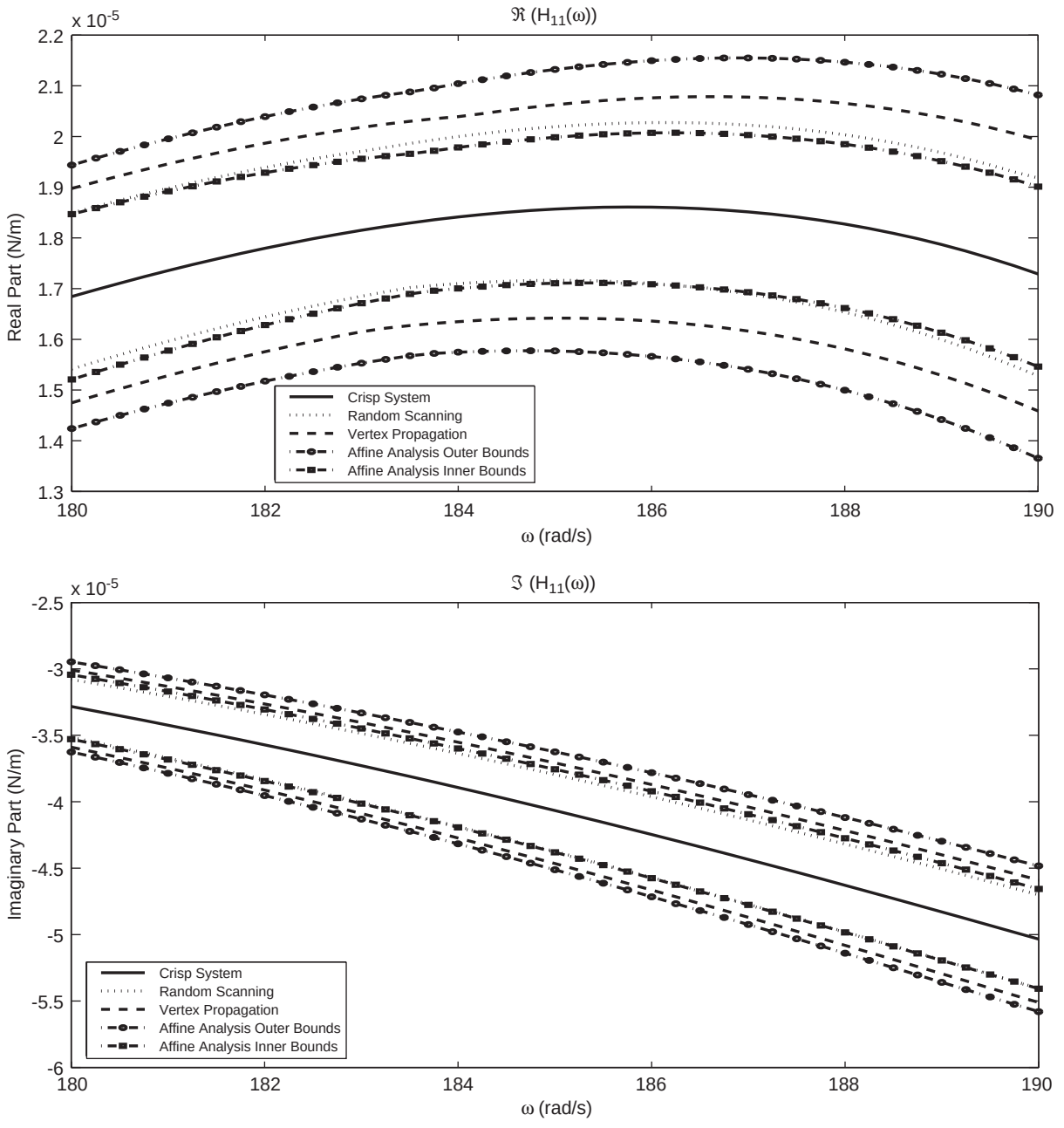

Fig. 18. Real and imaginary components of $H_{11}(\omega)$ in frequency range 180–190 rad/s.

Finite element models often have very large numbers of degrees of freedom and one does not have access to analytical expression of the crisp FRFs. It should be made clear that the FRF analysis approach via complex affine arithmetic demonstrated in the simple example will not be applicable for models of such complexity. The approach that is currently being investigated by the

author to incorporate the power of affine arithmetic into Finite Element methods is based around the modal superposition procedure as used by Moens [2]. It is anticipated that the affine arithmetic approach may be able to replace the optimisation stage for calculating the uncertain modal parameters whilst also keeping track of dependencies in the subsequent stages of the procedure thus resulting in computationally efficient, tight bounds on FRFs for complex structures with many parameters. Results will be reported shortly.

It should be stated that it is unlikely that these methods will be suitable for highly nonlinear systems. Iterative procedures will generally be required to solve such problems and care should be taken when simply *translating* deterministic algorithms for direct affine counterparts. It is very likely in such cases that the approximation errors will explode, albeit at a slower rate than would be expected using an interval arithmetic translation. Once again, this may be avoided by simply examining the size of the output approximation errors at each iteration.

7. Conclusions

This paper presented an alternative to complex interval analysis based around an extension of the Comba and Stolfi's real affine arithmetic [15] to the complex plane. Comparison of basic arithmetic operations conducted within the two frameworks illustrated the extra dimension of improvement available through the use of complex affine arithmetic over its interval counterpart. Whilst real affine arithmetic required there to be some relationship between operands in order to improve upon real interval arithmetic, complex affine arithmetic is able to offer the added advantage of describing the relationship between the real and imaginary solution components even if there is no dependency between the operands (or even between either operand's components).

In the more complicated situation of the frequency response functions of a 2 dof system with uncertain parameters, the complex affine analysis performed significantly better than its interval counterpart. That said, if the degree of assumed uncertainty were to be increased significantly, both methods would return worse predictions, as overestimations and approximation errors would increase considerably. This problem could be alleviated by performing several sub-analyses [16].

Affine arithmetic has three main advantages over interval arithmetic. The first is that it returns significantly tighter bounds on the true solution set. The second is that sensitivity information is returned by affine arithmetic relating to each independent source of uncertainty. The third advantage is the measure of usefulness of the prediction via examination of approximation errors which permit the calculation of inner and outer bounds between which the true solution set boundaries must lie.

It was stated that care must be taken when considering which procedures may be amenable to an affine translation in order to permit the concept of uncertainty into the analysis. Whereas it is expected that low-order systems (linear and weakly nonlinear), whose crisp FRFs may be obtained analytically, and linear finite element models may benefit from these techniques, it is not expected that algorithms requiring large numbers of iterative operations will return useful results, using this approach.

The possible uses for affine analysis (real and complex) fall into two camps. Firstly, those applications where interval analysis has been disregarded as a tool for dealing with uncertainty due its conservative nature and secondly, those applications where interval analysis is presently

used but dependency issues, perhaps weak, exist. One example of this second type may be fuzzy finite element analysis (e.g. [2]) which employs interval arithmetic for alpha-cuts of the membership function. Work has recently been published regarding the use of affine arithmetic representations of alpha-cuts for fuzzy arithmetic [18] and this will soon be extended to include fuzzy complex arithmetic.

Acknowledgements

The author would like to thank the referees for their extremely useful comments and suggestions.

References

[1] O. Dessombz, F. Thouverez, J.-P. Laîné, J. Jézéquel, Analysis of mechanical systems using interval computations applied to finite element methods, *Journal of Sound and Vibration* 239 (5) (2001) 949–968.
[2] D. Moens, A non-probabilistic finite element approach for structural dynamic analysis with uncertain parameters, Ph.D. Thesis, Katholieke Leuven, 2002.
[3] M. Hanss, The transformation method for the simulation and analysis of systems with uncertain parameters, *Fuzzy Sets and Systems* 130 (3) (2002) 277–289.
[4] W. Dong, H.C. Shah, Vertex method for computing functions of fuzzy variables, *Fuzzy Sets and Systems* 24 (1987) 65–78.
[5] K.L. Wood, K.N. Otto, E.K. Antonsson, Engineering design calculations with fuzzy parameters, *Fuzzy Sets and Systems* 52 (1992) 1–20.
[6] W. Dong, F.S. Wong, Fuzzy weighted averages and implementation of the extension principle, *Fuzzy Sets and Systems* 21 (1987) 183–199.
[7] R.E. Moore, Automatic error analysis in digital computation, Technical Report for Lockheed Missiles and Space Co. LMSD84821, 1959.
[8] R.E. Moore, Interval arithmetic and automatic error analysis in digital computing, Ph.D. Dissertation, Department of Mathematics, Stanford University, 1962.
[9] R.E. Moore, *Interval Analysis*, Prentice-Hall, Englewood Cliffs, NJ, 1966.
[10] R.E. Moore, *SIAM studies in applied mathematics*, Methods and Applications of Interval Analysis, 1979.
[11] R.B. Kearfott, M.T. Nakao, A. Neumaier, S.M. Rump, S.P. Shary, P. Van Hentenryck, Standardized notation in interval analysis, *Reliable Computing*, submitted, 2004.
[12] R.L. Muhanna, R.L. Mullen, Uncertainty in mechanics problems—interval-based approach, *Journal of Engineering Mechanics* 127 (6) (2001) 557–566.
[13] E.R. Hansen, Sharpness in interval computations, *Reliable Computing* 3 (1997) 17–29.
[14] R.E. Boche, Complex interval arithmetic with some applications, Technical Report for Lockheed Missiles and Space Division LMSC422661, 1965. Available at http://interval.louisiana.edu/Moores_early_papers/Boche_complex.pdf
[15] J.L.D. Comba, J. Stolfi, Affine arithmetic and its applications to computer graphics, *Proceedings of SIBGRAPI'93*, Brazil, 1993.
[16] G. Manson, Analysis of mechanical systems with uncertain parameters using affine analysis, *Journal of Sound and Vibration*, submitted, 2004.
[17] J. Stolfi, L.H. De Figueirido, Self-validated numerical methods and applications, *Monograph for 21st Brazilian Mathematics Colloquium*, 1997.
[18] G. Manson, Dependent alpha-cuts for fuzzy numbers using affine arithmetic, *Proceedings of NAFIPS 2003 Conference*, Chicago, IL, 2003.